

## RESEARCH ARTICLE



WILEY

# FMRF-NH<sub>2</sub>-related neuropeptides in *Biomphalaria* spp., intermediate hosts for schistosomiasis: Precursor organization and immunohistochemical localization

Solymar Rolón-Martínez<sup>1</sup> | Mohamed R. Habib<sup>2</sup> | Tamer A. Mansour<sup>3,4</sup> |  
 Manuel Díaz-Ríos<sup>5</sup> | Joshua J. C. Rosenthal<sup>6</sup> | Xiao-Nong Zhou<sup>7</sup> |  
 Roger P. Croll<sup>8</sup> | Mark W. Miller<sup>1</sup>

<sup>1</sup>Institute of Neurobiology and Department of Anatomy and Neurobiology, University of Puerto Rico, Medical Sciences Campus, San Juan, Puerto Rico

<sup>2</sup>Medical Malacology Laboratory, Theodor Bilharz Research Institute, Giza, Egypt

<sup>3</sup>Department of Population Health and Reproduction, School of Veterinary Medicine, University of California, Davis, California, USA

<sup>4</sup>Department of Clinical Pathology, School of Medicine, University of Mansoura, Mansoura, Egypt

<sup>5</sup>Department of Biology, Bowdoin College, Brunswick, Maine, USA

<sup>6</sup>Marine Biological Laboratory, Woods Hole, Massachusetts, USA

<sup>7</sup>National Institute of Parasitic Diseases, Chinese Center for Disease Control and Prevention, Shanghai, People's Republic of China

<sup>8</sup>Department of Physiology and Biophysics, Dalhousie University, Halifax, Nova Scotia, Canada

## Correspondence

Mark W. Miller, Institute of Neurobiology, University of Puerto Rico, 201 Blvd del Valle, San Juan 00901, Puerto Rico.  
 Email: mark.miller@upr.edu

## Funding information

Division of Biological Infrastructure, Grant/Award Numbers: DBI-0932955, DBI-1337284; Division of Human Resource Management, Grant/Award Number: HRD-1137725; National Academy of Sciences, Grant/Award Number: 2000007152; National Center on Minority Health and Health Disparities (National Institutes of Health), Grant/Award Number: U54 MD007600; National Institute of General Medical Sciences, Grant/Award Numbers: P20 GM103475, P20 GM103642, R25 GM061838; Office of International Science and Engineering, Grant/Award Number: OISE-1545803; Science and Technology Development Fund, Grant/Award Number: USC17-188

## Abstract

Freshwater snails of the genus *Biomphalaria* serve as intermediate hosts for the digenetic trematode *Schistosoma mansoni*, the etiological agent for the most widespread form of intestinal schistosomiasis. As neuropeptide signaling in host snails can be altered by trematode infection, a neural transcriptomics approach was undertaken to identify peptide precursors in *Biomphalaria glabrata*, the major intermediate host for *S. mansoni* in the Western Hemisphere. Three transcripts that encode peptides belonging to the FMRF-NH<sub>2</sub>-related peptide (FaRP) family were identified in *B. glabrata*. One transcript encoded a precursor polypeptide (*Bgl-FaRP1*; 292 amino acids) that included eight copies of the tetrapeptide FMRF-NH<sub>2</sub> and single copies of FIRF-NH<sub>2</sub>, FLRF-NH<sub>2</sub>, and pQFYRI-NH<sub>2</sub>. The second transcript encoded a precursor (*Bgl-FaRP2*; 347 amino acids) that comprised 14 copies of the heptapeptide GDPFLRF-NH<sub>2</sub> and 1 copy of SKPYMRF-NH<sub>2</sub>. The precursor encoded by the third transcript (*Bgl-FaRP3*; 287 amino acids) recapitulated *Bgl-FaRP2* but lacked the full SKPYMRF-NH<sub>2</sub> peptide. The three precursors shared a common signal peptide, suggesting a genomic organization described previously in gastropods. Immunohistochemical studies were performed on the nervous systems of *B. glabrata* and *B. alexandrina*, a major intermediate host for *S. mansoni* in Egypt. FMRF-NH<sub>2</sub>-like immunoreactive (FMRF-NH<sub>2</sub>-li) neurons were located in regions of the central nervous system associated with reproduction, feeding, and cardiorespiration. Antisera raised against non-FMRF-NH<sub>2</sub> peptides present in the tetrapeptide and heptapeptide precursors labeled independent subsets of the FMRF-NH<sub>2</sub>-li neurons. This study supports the participation of FMRF-NH<sub>2</sub>-related neuropeptides in the regulation of vital physiological and behavioral systems that are altered by parasitism in *Biomphalaria*.

## KEYWORDS

*Biomphalaria alexandrina*, *Biomphalaria glabrata*, neuropeptides, pond snail, pulmonate mollusk, *Schistosoma mansoni*

## 1 | INTRODUCTION

Schistosomiasis is a debilitating parasitic disease that impacts over 200 million people worldwide (World Health Organization [WHO] Global Health Observatory Data 2020). Globally, the most widespread form of human intestinal schistosomiasis is caused by the digenetic trematode *Schistosoma mansoni*. The complex life cycle of *S. mansoni* includes an obligatory intermediate snail host of the genus *Biomphalaria* (Class: Gastropoda; Family: Planorbidae; Maldonado & Perkins, 1967; Rollinson & Chappell, 2002; Toledo & Fried, 2011).

Schistosome parasites can promote their own survival, reproduction, and growth by altering neuropeptide signaling in their intermediate hosts (de Jong-Brink, 1995; de Jong-Brink et al., 2001; Hoek et al., 2005). One such neuropeptide, FMRF-NH<sub>2</sub>, initially identified in the clam *Macrocallista nimbosa* (Price & Greenberg, 1977, 1989), has been intensively studied in gastropods (Cottrell, 1993; Santama & Benjamin, 2000; Zatylny-Gaudin & Favrel, 2014). FMRF-NH<sub>2</sub>-related peptides (FaRPs) modulate neural activity and synaptic transmission within gastropod central nervous systems (Baux et al., 1992; Brezina et al., 1987; Cottrell et al., 1992; Mackey et al., 1987; Man-Song-Hing et al., 1989). Peripheral functions include regulation of muscle contraction (Austin et al., 1983; Cottrell et al., 1983; Lehman & Greenberg, 1987) and cardioregulation (Alevizos et al., 1989; Buckett, Peters, & Benjamin, 1990; Buckett, Peters, Dockray, et al., 1990; Brezden et al., 1991). Central neurons that express FaRPs participate in the control of reproductive behaviors (Acker et al., 2019; Brussaard et al., 1988; van Golen et al., 1995) and feeding (Alania et al., 2004; Lloyd et al., 1987; Murphy, 1990; Vilim et al., 2010).

Due to the pleiotropic functions of the FaRPs in gastropods, this neuropeptide family is considered a potential target for schistosome larvae (de Jong-Brink, 1995; de Jong-Brink et al., 2001). In the host-parasite interaction between the pulmonate snail *Lymnaea stagnalis* and the avian schistosome *Trichobilharzia ocellata*, significant increases in FMRF-NH<sub>2</sub> gene expression were measured across the postinfection chronology (Hoek et al., 1997). The early onset of this increase (>300% at 5 h) was proposed to support a direct effect of parasitism on the host brain. Later increases (6 and 8 weeks post-infection) could contribute to the schistosome survival strategy during the shedding stage of infection, when host energy resources are redirected toward the large numbers of cercariae inhabiting the snail. Increased levels of FMRF-NH<sub>2</sub> were also detected in *Biomphalaria glabrata* at 12 days postinfection with *S. mansoni* (Wang et al., 2017).

The pivotal role of FaRPs in the regulation of physiological and behavioral systems in gastropods, coupled with findings that schistosome infection can alter host FMRF-NH<sub>2</sub> gene expression, stimulated the present characterization of FaRP encoding transcripts and precursor organization in *B. glabrata*. Antisera generated against the deduced peptide products were also used to localize expression of this neuropeptide family in the central nervous system circuits controlling physiological and behavioral functions that are impacted by parasitism.

## 2 | MATERIALS AND METHODS

### 2.1 | Specimens

Experiments on *B. glabrata* were performed at the University of Puerto Rico. The investigation was conducted on laboratory-bred snails that were maintained in aquaria at room temperature and fed lettuce *ad lib*. All protocols were approved by the Institutional Animal Care and Use Committee (IACUC) of the University of Puerto Rico Medical Sciences Campus (Protocol #3220110). Experiments on *B. alexandrina* were conducted at the National Institute of Parasitic Diseases, Chinese Center for Disease Control and Prevention, Shanghai, People's Republic of China on specimens collected from watercourses in Giza, Egypt. Snails of both species ranged from 8 to 15 mm in shell diameter.

### 2.2 | Transcriptomics

RNA was extracted from 12 pooled *B. glabrata* central nervous systems. Synthesis of cDNA was performed and RNAseq reads (Illumina HiSeq 2500) were generated by the Research Technology Support Facility of Michigan State University. Reads were assembled and annotated using the Eel Pond mRNAseq Protocol (<https://khmerprotocols.readthedocs.org/en/v0.8.4/mrna-seq/>). The assembly protocol involved clipping of Illumina adaptors by Trimmomatic (Bolger et al., 2014) and quality trimming of sequencing reads by FASTX-Toolkit ([http://hannonlab.cshl.edu/fastx\\_toolkit](http://hannonlab.cshl.edu/fastx_toolkit)). Additional k-mer-based trimming of erroneous sequences and digital normalization to minimize redundant sequences were done using Khmer software (Crusoe et al., 2015; Grabherr et al., 2011). Assembly was performed by Trinity software in two batches to avoid chimeric assemblies with a minimum contig length of 200 bp. *De novo* transcripts were aggregated into transcript families and functionally annotated by reciprocal sequence alignment against the refseq database of mouse proteins using BLAST (Altschul et al., 1990). The final assemblies produced by the Eel Pond protocol were pooled and CD-HIT (Li & Godzik, 2006) was used to deduplicate sequences with 95% similarity or more. As a quality control, Benchmarking Universal Single-Copy Orthologs (BUSCO v5.0.0) was used for quantitative assessment of the transcriptome completeness with automatic selection of the reference lineage using the auto-lineage-euk option (Seppey et al., 2019). Nucleotide sequences annotated as "FMRFamide neuropeptides" were translated using the ExPASy translate tool (Swiss Institute of Bioinformatics [SIB], Basel, Switzerland; <http://www.expasy.ch/tools/dna.html>). Signal peptide prediction was implemented with SignalP 4.1 (Center for Biological Sequence Analysis, Technical University of Denmark, Lyngby, Denmark; <http://www.cbs.dtu.dk/services/SignalP/>; Petersen et al., 2011). Precursor cleavage sites and posttranslational modifications were predicted using the ProP 1.0 server (<http://www.cbs.dtu.dk/services/ProP/>) and comparison with precursors characterized in other gastropods (Kellett et al., 1994; Lutz et al., 1992; Saunders et al., 1991, 1992).

## 2.3 | Whole-mount immunohistochemistry

Standard whole-mount immunohistochemical protocols were followed (see Beach et al., 2019; Rosa-Casillas et al., 2021; Vaasjo et al., 2018). Dissections were performed in normal saline (in mmol L<sup>-1</sup>: NaCl 51.3, KCl 1.7, MgCl<sub>2</sub> 1.5, CaCl<sub>2</sub> 4.1, HEPES 5, pH 7.8.), and pinned in a Sylgard plate. Ganglia were incubated in protease (0.5%; Type VI, Sigma; 10–15 min), washed thoroughly with normal saline, and then fixed in cold 4% paraformaldehyde prepared in 80 mM phosphate buffer (PB: 24 mM KH<sub>2</sub>PO<sub>4</sub>, 56 mM Na<sub>2</sub>HPO<sub>4</sub>, pH 7.4) containing 24% sucrose. Following fixation, tissues were washed 5 × 20 min in PTA (0.1 M PB containing 2% Triton X-100 and 0.1% sodium azide) at room temperature. Following preincubation with normal goat (NGS) or donkey serum (NDS, 0.8%), tissues were immersed (2–4 days, room temperature) in one or more of the following primary antibodies: (1) FMRF-NH<sub>2</sub> rabbit polyclonal antiserum (1:1000 dilution; Immunostar Catalog Number 20091; RRID AB\_572232; raised against FMRF-NH<sub>2</sub> coupled to bovine thyroglobulin), (2) *Bgl-FaRP1* specific goat polyclonal antiserum (1: 4000 dilution; Capralogics Inc., Hardwick MA; raised against C-SDQPDVDDYIRA coupled to BSA), (3) *Bgl-FaRP2* and *Bgl-FaRP3* (*Bgl-FaRP2/3*) specific sheep polyclonal antiserum (1:1000 dilution; Capralogics Inc.; raised against C-FKPPTDTEDNSIDLDDDEDIS coupled to BSA).

Following repeated PTA washes (×5, at least 20 min each, room temperature), tissues were incubated in secondary antibodies conjugated to a fluorescent marker (Alexa 488 goat anti-rabbit IgG [H + L] conjugate; Alexa 488 donkey anti-rabbit IgG [H + L] conjugate; Alexa 546 donkey anti-rabbit IgG [H + L] conjugate; Alexa 488 donkey anti-goat IgG [H + L] conjugate; Alexa 546 donkey anti-sheep IgG [H + L] conjugate; Molecular Probes, Eugene OR) at dilutions ranging from 1:500 to 1: 4000.

Quality of the staining was assessed using a Nikon Eclipse fluorescence microscope prior to imaging. Confocal imaging was performed on a Nikon A1R Confocal Laser Microscope using the NIS Elements AR (Version. 4.5, Nikon Instruments) or a Zeiss Laser Scanning Confocal Microscope (Pascal LSCM) using the Zeiss LSM 5 Image Browser (Version 3.1.0.11). Stacks, z-series, overlays, and calibrations were obtained using the Fiji software (v. 2.00, NIH public domain). Graphs and schematics were edited or created using the Prism Software or EazyDraw 8 software v. 8.3.0 (Dekorra Optics LCC, Poynette, WI). Images were edited using the Fiji software, as well as the GNU Image Manipulation Program (GIMP) software v. 2.8.16 (Free Software Foundation, Inc.), and EazyDraw 8 software for addition of labels and organization of panels.

### 2.3.1 | Antibody characterization

The pattern of staining produced by the commercial FMRF-NH<sub>2</sub> antibody was in general agreement with previous observations in numerous gastropods (e.g., Acker et al., 2019; Boer et al., 1980; Cardot & Fellman, 1983; Cooke & Gelperin, 1988; Elekes & Ude, 1994; Lehman & Price, 1987; Lloyd et al., 1987; Schot & Boer, 1982). The FMRF-NH<sub>2</sub> antibody reacts with both tetrapeptide and extended FaRPs,

requiring only a C-terminal aromatic amino acid, a penultimate arginine residue, and a total length of at least four residues (Greenberg et al., 1988). The non-FaRP antibodies only labeled subsets of the FMRF-NH<sub>2</sub>-li neurons, in a pattern that resembled observations in *L. stagnalis* and *Helix aspersa* (MacDonald et al., 1994; Santama et al., 1993, 1996). Specificity of the *Bgl-FaRP1* antibody was also supported by *in situ* hybridization experiments using a probe against the corresponding message (Figures 10(d), 11(e), and 12(d)). Negative control experiments conducted with all antibodies included (1) omission of each primary antibody, and (2) omission of each secondary antibody. Signals were also eliminated when the *Bgl-FaRP1* and *Bgl-FaRP2* antibodies were preabsorbed with the peptides that were used for their production ( $3 \times 10^{-4}$  M, overnight). Attempts to use the *Bgl-FaRP1* and *Bgl-FaRP2/3* antibodies for simultaneous detection of neurons that express distinct precursors were unsuccessful. This limitation probably reflected the close relationship between the Caprinae hosts (goat and sheep) in which the antibodies were generated.

## 2.4 | Nerve backfills

The biotin-avidin protocol followed methods described previously (Delgado et al., 2012; Vallejo et al. 2014). Briefly, the central nervous system was dissected in normal saline and the nerve of interest was pinned out near a small well that was formed from petroleum jelly (Vaseline) on the surface of a Sylgard-lined petri dish. The nerve being examined was then cut and drawn into the well. Care was taken to avoid contact between the end of the nerve and the Vaseline. The tip of the nerve was cut one more time and then the snail saline inside the well was withdrawn and replaced with a saturated aqueous solution (1.4 mg/50 µl) of biocytin (Sigma Chemical, St. Louis, MO). The walls of the well were then built up with successive layers of Vaseline, effectively isolating the biocytin pool from the saline surrounding the ganglion. The preparation was covered and incubated overnight at 4°C. Following incubation, the well was removed, and ganglia washed three to five times, repinned, incubated in protease (0.5%, 10–12 min), and fixed in 4% paraformaldehyde for 1 h at room temperature. Fixed ganglia were transferred to microcentrifuge tubes, washed five times (20 min each) with PTA solution and incubated overnight (room temperature) in Alexa Avidin 546 (Vector Laboratories, Burlingame, CA) diluted 1:400 in PTA (24–48 h, room temperature) or Streptavidin Pacific Blue (Molecular Probes) diluted by a factor of 1:500 in PTA (24–48 h at room temperature). The quality of the backfill was assessed daily using a Nikon Eclipse fluorescence microscope prior to further immunohistochemical processing. Once the backfill was determined to be of sufficient quality, preparations were processed with a standard immunohistochemical procedure as described above. Some ganglia processed for penial nerve backfills were treated with 4',6-diamidino-2-phenylindole (DAPI) nuclear counterstaining to quantify the total number of neurons located in the ventral lobe. Preparations were incubated in VECTASHIELD Antifade Mounting Medium with DAPI (1.5 µg/ml; Vector Laboratories, product H-1200) for at least 72 h prior to imaging.

## 2.5 | Whole-mount fluorescence *in situ* hybridization

As *Bgl-FaRP1* and *Bgl-FaRP2/3* could not be detected simultaneously (see previous text), whole-mount *in situ* hybridization for the

*Bgl-FaRP1* precursor was used to substantiate immunohistochemical observations. A 48-mer antisense oligonucleotide probe, corresponding to nucleotides 566–613 (encoding amino acids 92–107 of *Bgl-FaRP1*; Figure 1(a), *dashed line*), was synthesized by Integrated DNA Technologies (Coralville, IA). A sense probe corresponding to the same

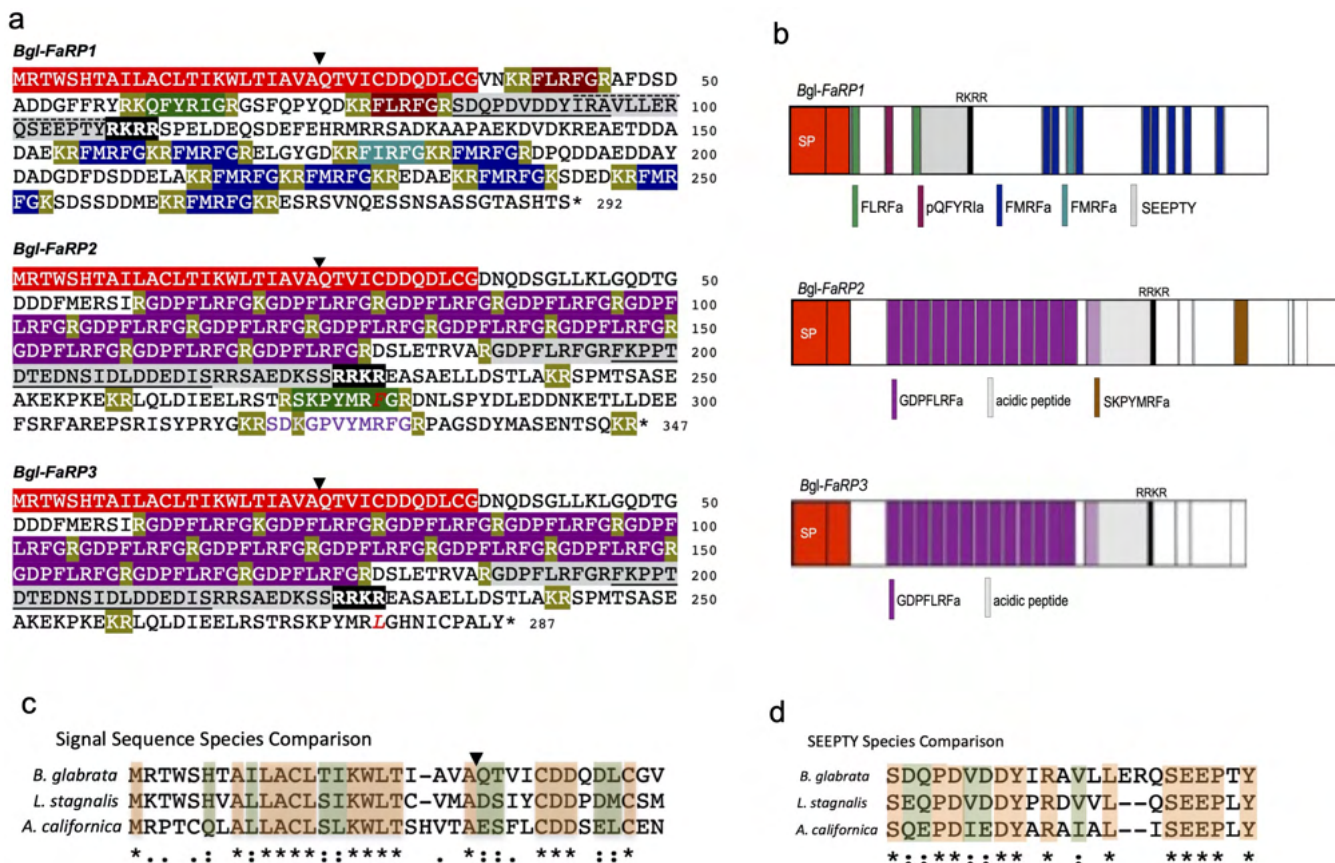


**FIGURE 1** The *Biomphalaria glabrata* FMRP-NH<sub>2</sub>-related peptide (FaRP) precursors. (a) Amino acid sequences of three FaRP precursors predicted from a *B. glabrata* CNS transcriptome. Top: *Bgl-FaRP1* was deduced from two partial transcripts, biomph.id56759.tr165475 (967 nucleotides) and biomph.id58929.tr190947 (986 nucleotides), with 212 nucleotides overlap. The ORF encoded the *Bgl-FaRP1* precursor (292 amino acids) from which the tetrapeptides FLRF-NH<sub>2</sub> (green highlight, white text), FMRF-NH<sub>2</sub> (dark blue highlight, white text), FIRF-NH<sub>2</sub> (teal highlight, white text), and the pentapeptide pQFYRI-NH<sub>2</sub> (maroon highlight, white text) could be liberated. Potential cleavage sites are highlighted olive (white text). The SignalP-5.0 algorithm predicted signal peptide cleavage following the alanine at position 23 (downward arrowhead; likelihood = 0.9485). The initial 35 amino acids (red highlight, white text) were shared by all three precursors. The sequence used to generate a *Bgl-FaRP1*-specific antibody (SDQPDVDDYIRAVLLERQSEETTY) is underlined and a dashed line is drawn over the sequence (IRAVLLERQSEETTY) corresponding to the oligonucleotide probe used for *in situ* hybridization. A furin proprotein convertase site, RKRR, is located at positions 108–111 (black highlight, white text). Middle: The *Bgl-FaRP2* (347 amino acids) precursor was deduced from a single full-length transcript (biomph.id35970.tr258599; 1772 nucleotides). The SignalP-5.0 algorithm predicted signal peptide cleavage following the alanine at position 23 (downward arrowhead; likelihood = .0.9719). Fourteen copies of the heptapeptide GDPFLRF-NH<sub>2</sub> (purple highlight, white text) and one copy of SKPYMRF-NH<sub>2</sub> (tan highlight, brown text) could be liberated from the *Bgl-FaRP2* precursor. The sequence used to generate a *Bgl-FaRP2/3*-specific antibody (FKPPTDTEDNSIDLDD~~EDIS~~) is underlined and the RKRR furin cleavage site (aa 225–228) is highlighted black (white text). The phenylalanine residue in position 278 (italicized, red text) signifies the divergence between the *Bgl-FaRP2* and *Bgl-FaRP3* precursors. Bottom: The *Bgl-FaRP3* precursor is deduced from a single full-length transcript (biomph.id35966.tr258599; 2060 nucleotides) with a 833 nucleotide overlap with biomph.id35970.tr258599. The Leu<sub>278</sub> residue, where the *Bgl-FaRP3* precursor diverges from *Bgl-FaRP2*, is shown in italicized red text. (b) Schematic representations of the three FaRP precursors. The shared sequence (red) includes the signal peptide (SP). *Bgl-FaRP1* gives rise to three distinct FaRP tetrapeptides and one pentapeptide (color codes shown below each schematic). The *Bgl-FaRP2* and *Bgl-FaRP3* precursors contain FaRP heptapeptides. The heptapeptide SKPYMRF-NH<sub>2</sub>, which is present in *Bgl-FaRP2*, is truncated in *Bgl-FaRP3*. Vertical lines denote potential basic and dibasic cleavage sites. (c) The proposed signal sequence of the *B. glabrata* precursors (21 residues) exhibited conservation with the signal sequences of FMRF-NH<sub>2</sub> precursors of *L. stagnalis* (15 identical, 4 similar residues) and the more distantly related opisthobranch *Aplysia californica* (11 identical, 4 similar residues). Conservation remained high in the 13 residues following the signal peptide cleavage site (downward arrowhead) that originate from the first exon. Two cysteine and two aspartate residues were identical to the FaRP precursors of *L. stagnalis* and *A. californica*. (d) The SEEPTY peptide of the *B. glabrata* *Bgl-FaRP1* precursor exhibits a high degree of conservation with the corresponding peptides of *L. stagnalis* and *A. californica* [Color figure can be viewed at [wileyonlinelibrary.com](http://wileyonlinelibrary.com)]



sequence was tested as a control. Oligonucleotides were tailed (3' end, digoxigenin-dUTP) following the instructions of the kit manufacturer (DIG Oligonucleotide Tailing Kit, second generation; Roche Life Science U.S., Indianapolis, IN; Product Number 03353583910).

Dissection of the central nervous system was conducted in normal saline. Ganglia were fixed with cold 4% paraformaldehyde for 1 h followed by  $5 \times 15$  min washes in PTA. Tissues were then incubated in Proteinase K (Thermo Scientific) 5 µg/ml PTA for approximately 30 min or until the ganglia edges began to appear slightly translucent. Ganglia were then washed  $3 \times 15$  min in PTA. Postfixation (30 min with 4% paraformaldehyde) was followed with  $2 \times 15$  min washes in a glycine solution (2 mg/ml PTA). Tissues were then transferred to microcentrifuge tubes and prehybridized at 34°C with shaking for 1 h in hybridization buffer (50% formamide, 5 mM EDTA,  $\times 5$  saline-sodium citrate [SSC],  $1 \times$  Denhardt's solution, 0.1% Tween-20, 0.5 mg/ml salmon sperm DNA). Following prehybridization, tissues were hybridized with the tailed oligonucleotide (1 µg/ml hybridization buffer) overnight at 34°C with shaking. Tissues were then washed  $3 \times 30$  min in a  $2 \times$  SSC/0.01% sodium dodecyl sulfate solution at 34°C, followed by  $2 \times 10$  min washes with PTA and block with NGS or NDS (0.8% in PTA) for at least 3.5 h. Following blocking, samples were incubated in a digoxigenin antibody, ABfinity rabbit oligoclonal (Life Technologies, Carlsbad, CA; catalog number 9HCLC) at a dilution of 1:500 overnight at room temperature. Excess antibody was removed with  $5 \times 15$  min PTA washes, followed by incubation with a second antibody conjugated to a fluorescent marker (Alexa 488 goat anti-rabbit IgG [H + L] or Alexa 488 donkey anti-rabbit IgG [H + L]; Molecular Probes). Hybridization was assessed with a Nikon Eclipse fluorescence microscope prior to confocal imaging.

### 3 | RESULTS

#### 3.1 | *B. glabrata* transcriptome

The assembled transcriptome had 180,829 transcripts with a total size of ~134.6 MB and an N50 of 1291 bp. The longest assembled transcript was ~17.2 kb while the average length of all transcripts was ~744 bp. The whole transcriptome, not filtered for isoforms, was subjected to translate BLAST and hidden Markov model searches against OrthoDB's sets of BUSCO of eukaryotes. This analysis estimated the predicted protein-coding gene set to be 96.5% complete (64.3% with single-copy BUSCOs and 32.2% with duplicated BUSCOs) based on eukaryota\_odb10 BUSCO families. Automatic phylogenetic placement among the eukaryotic datasets identified the mollusca dataset as the best matching group and showed 85.0% completeness (67.0% with single-copy BUSCOs and 18.0% with duplicated BUSCOs) based on mollusca\_odb10 BUSCO family.

#### 3.2 | The *B. glabrata* FaRP transcripts

Annotation of a *B. glabrata* neural transcriptome identified three cDNAs with significant homology to transcripts that encode FaRP

precursors in other gastropods (Figure 1). One cDNA, 1758 base pairs in length (GenBank accession: MW387019.1), contained an open reading frame (ORF; 876 nucleotides) that was preceded by a 292 nucleotide 5' untranslated sequence and followed by 590 nucleotides of 3' untranslated sequence. A BLAST performed with NCBI databases identified a genomic sequence (ref|XM\_013210814.1; PREDICTED: *B. glabrata* FMRF-amide neuropeptides-like [LOC106054785], mRNA) with 98% identity between nucleotides 393–1172 of this transcript. BLAST queries for nucleotides 1–392 and 1173–1758 did not produce matching sequences. The sequence of the 292 amino acid *B. glabrata* FMRF-NH<sub>2</sub>-related peptide precursor 1 (termed *Bgl-FaRP1*; Figure 1(a,b)) was nearly identical to the FMRF-NH<sub>2</sub> precursor previously mined from *B. glabrata* genomic and transcriptomic data (Adema et al., 2017; Wang et al., 2017). It differed at only six residues, none of which occurred within the sequences of the final predicted peptide products.

A second transcript, 1772 nucleotides in length (GenBank accession: MW825357), encoded a full-length precursor containing sequences for FMRF-NH<sub>2</sub>-related heptapeptides. A portion of this transcript (nucleotides 547–1772) also shared significant (97%) identity with the NCBI XM\_013210814 genomic sequence, with no NCBI sequences corresponding to nucleotides 1–546. The longest ORF encoded a 347 amino acid preprohormone, designated *B. glabrata* FaRP precursor 2 (*Bgl-FaRP2*; Figure 1(a,b)).

Nucleotides 155–546 of the *Bgl-FaRP2* transcript, which includes the initial 103 nucleotides of the deduced ORF, were identical to nucleotides 1–392 of the *Bgl-FaRP1* transcript. The shared 5' sequence of the two transcripts was indicative of alternative splicing, as occurs in FaRP transcripts of the pulmonates *L. stagnalis* and *H. aspersa*, and the vetigastropod *Haliotis asinina* (Cummins et al., 2011; Lutz et al., 1992; Saunders et al., 1992).

A third transcript, 2060 nucleotides in length (GenBank accession: MW387020.1), shared its initial 1272 nucleotides with the *Bgl-FaRP2* transcript. It then diverged, reaching a termination codon after 28 nucleotides. The ORF of this transcript encoded a precursor, termed *Bgl-FaRP3*, 287 amino acids in length (Figure 1(a,b)). It was preceded by 440 of 5' untranslated nucleotides and followed by 696 nucleotides of 3' untranslated sequence including three consensus signals (two AAUAAA, one AUUAAA) for polyadenylation (Proudfoot & Brownlee, 1976).

#### 3.3 | The *B. glabrata* FaRP precursors

The SignalP-5.0 algorithm (Almagro Armenteros et al., 2019) yielded a prediction for signal peptide cleavage following the alanine at position 23 of the FaRP precursors (Figure 1(a,b)). Signal peptide cleavage is thus proposed to occur within the N-terminal region that is shared by the three precursors. The sequence of the proposed leader sequence (21 residues) exhibited conservation with the signal sequences of FMRF-NH<sub>2</sub> precursors of *L. stagnalis* (15 identical, 4 similar residues) and the more distantly related opisthobranch *Aplysia californica* (11 identical, 4 similar residues; Figure 1(c)). This conserved sequence remained high through the shared initial portion of the prohormones,

in which two cysteine and two aspartate residues were identical to the FaRP precursors of *L. stagnalis* and *A. californica* (Figure 1(c)).

A canonical furin proprotein convertase site, RKRR (Hosaka et al., 1991), was present at positions 108–111 of the *Bgl-FaRP1* precursor (Figure 1(a,b)). Furin cleavage may enable differential sorting and trafficking of the peptide subsets located N-terminal and C-terminal from this tetrapeptide sequence (see Fisher et al., 1988; Li et al., 1994; Sossin et al., 1990; Sweet-Cordero et al., 1990). Three FaRPs were encoded between the N-terminus of the precursor and the tetrabasic site, two copies of FLRFG (aa 40–44 and 78–82) and one copy of QFYRIG (aa 61–66). Cleavage and posttranslational processing of the N-terminus portion of the precursor will thus result in two copies of FLRF-NH<sub>2</sub> and one copy of the pentapeptide pQFYRI-NH<sub>2</sub>. The segment of the *Bgl-FaRP1* precursor between the furin cleavage site and the carboxyl terminus consists of a repeating motif of FaRPs alternating with acidic spacer regions of varying length. The C-terminal FaRPs, all tetrapeptides, include eight copies of FMRF-NH<sub>2</sub> and one FIRF-NH<sub>2</sub>.

In *L. stagnalis*, a 22 amino acid peptide, termed “SEEPLY” due to its C-terminal sequence, was purified and shown to exist as a steady-state final product of the tetrapeptide precursor (Santama et al., 1993). The sequence located between Arg<sub>83</sub> and the tetrapeptide furin signal of the *Bgl-FaRP1* (shaded gray in Figure 1(a,b); designated SEEPTY) exhibited substantial conservation with the SEEPLY peptides of *L. stagnalis* and *A. californica* (Figure 1(d)). A portion of the SEEPTY peptide, underlined in Figure 1(a), was used to generate a *Bgl-FaRP1* specific antibody (see Section 2).

The *Bgl-FaRP2* and *Bgl-FaRP3* precursors also contain a furin signal (RRKR; aa 225–228) that could produce an initial *trans*-Golgi cleavage. The segment of the precursor between the signal peptide and the tetrabasic sequence comprises 14 copies of the heptapeptide GDPFLRF-NH<sub>2</sub>. In *L. stagnalis*, cleavage at the carboxyl arginine of the ultimate heptapeptide does not occur, resulting in a long “acidic peptide” product that includes this FaRP sequence and extends to the furin tetrapeptide (Santama et al., 1996; see below). Immunohistochemical observations using an antibody against a region of the *Bgl-FaRP2/3* acidic peptide (underlined in Figure 1(a)) were consistent with similar processing in *B. glabrata*. A single copy of SKPYMRF-NH<sub>2</sub> was present in the C-terminal region of *Bgl-FaRP2* following the furin signal. Additional monobasic and dibasic residues present within the C-terminal could result in additional RF-NH<sub>2</sub> peptides (GPVYMRF-NH<sub>2</sub>, SDKGPVYMRF-NH<sub>2</sub>; Figure 1(a), purple text). However, potential peptide products in the corresponding region of the *Lymnaea* heptapeptide precursor were not detected by mass spectrometry (Kellett et al., 1994; Worster et al., 1998).

The *Bgl-FaRP3* precursor diverged from *Bgl-FaRP2* following Arg<sub>277</sub> (Figure 1(a)). The *Bgl-FaRP3* precursor extended 10 additional amino acids beginning with Leu-Gly-His. The SKPYMRFGR of *Bgl-FaRP2* is thus modified to a sequence, SKPYMRLGH, that lacks consensus residues for cleavage or amidation (Figure 1(a)). In *L. stagnalis*, a splice site is located within the codon for the Arg<sub>6</sub> of SKPYMRF-NH<sub>2</sub> of the heptapeptide FaRP precursor, but there is no evidence for the occurrence of alternative splicing at this site (Kellett et al., 1994; see Section 4).

### 3.4 | Localization of FMRF-NH<sub>2</sub>-like immunoreactivity in the central nervous system

Whole-mount immunohistochemical experiments labeled neurons in the central nervous systems of both *B. glabrata* and *B. alexandrina* (Figure 2). Cell distributions and sizes were indistinguishable between the species. Neurons were located in all central ganglia, with cell bodies located on the dorsal and ventral surfaces of the CNS. The distribution of FMRF-NH<sub>2</sub>-li cells was consistent with the involvement of this peptide family in the regulation of diverse physiological and behavioral functions related to reproduction, feeding, and cardiorespiration.

#### 3.4.1 | Reproduction

In sinistral pulmonates, central neurons with projections to the penial nerve include: (1) the ventral lobe (V l.) in the left cerebral hemiganglion (Figures 2 and 3(a–f)), (2) the anterior lobe of the left cerebral ganglion, (3) a cluster of approximately 15–20 neurons in the Pdlb cluster of the left pedal ganglion (Figure 3(g–i); see Delgado et al., 2012), (4) dispersed neurons in the left pleural ganglion (Figure 6), and (5) two clusters of cells in the left parietal ganglion (Figure 6).

As reported previously by Acker et al. (2019), FMRF-NH<sub>2</sub>-li cells were located in the ventral lobe of the left cerebral hemiganglion, a lateralized cluster of neurons associated with innervation of male reproductive structures (Li & Chase, 1995; van Golen et al., 1995; Koene et al., 2000). FMRF-NH<sub>2</sub>-li cells ( $90.6 \pm 22.4$ ,  $n = 3$ ) in the ventral lobe of *B. glabrata* ranged in diameter from 5 to 25  $\mu$ m (Figure 2(a,b)). FMRF-NH<sub>2</sub>-li fibers coursed through the cerebral ganglia, with prominent projections in the cerebral commissure (C c.; Figure 2(a,c)). FMRF-NH<sub>2</sub>-li fiber tracts were also present in the cerebral-buccal connectives, the cerebral-pedal connectives, and the cerebral-pleural connectives.

The abundance of FMRF-NH<sub>2</sub>-li neurons in the ventral lobe prompted double-labeling (penis nerve retrograde biocytin tracing  $\times$  FMRF-NH<sub>2</sub>-like immunoreactivity) experiments to localize central FaRP expressing neurons that project toward the male reproductive structures. Relatively few ( $11.6 \pm 2.0$ ,  $n = 3$ ) of the FMRF-NH<sub>2</sub>-li neurons were also labeled with backfills of the penis nerve (Figure 3(f)). In the pedal ganglia, FMRF-NH<sub>2</sub>-li cells were observed in the region of the Pdlb cluster (Figure 3(h)), but close examination showed that none of the biocytin-labeled neurons exhibited FMRF-NH<sub>2</sub>-like immunoreactivity (Figure 3(i)).

The potential involvement of FaRPs in the regulation of male mating behavior was further examined using antibodies that could distinguish between the FaRP precursors. A goat antiserum was produced against a region of the *Bgl-FaRP1* SEEPTY peptide (SDQPDVD DYIRA; underlined in Figure 1(a); Materials and Methods). All ventral lobe neurons labeled with this antibody also exhibited FMRF-NH<sub>2</sub>-like immunoreactivity, supporting its specificity as a marker for *Bgl-FaRP1* localization (Figure 4(a–c)). Experiments in which penis nerve

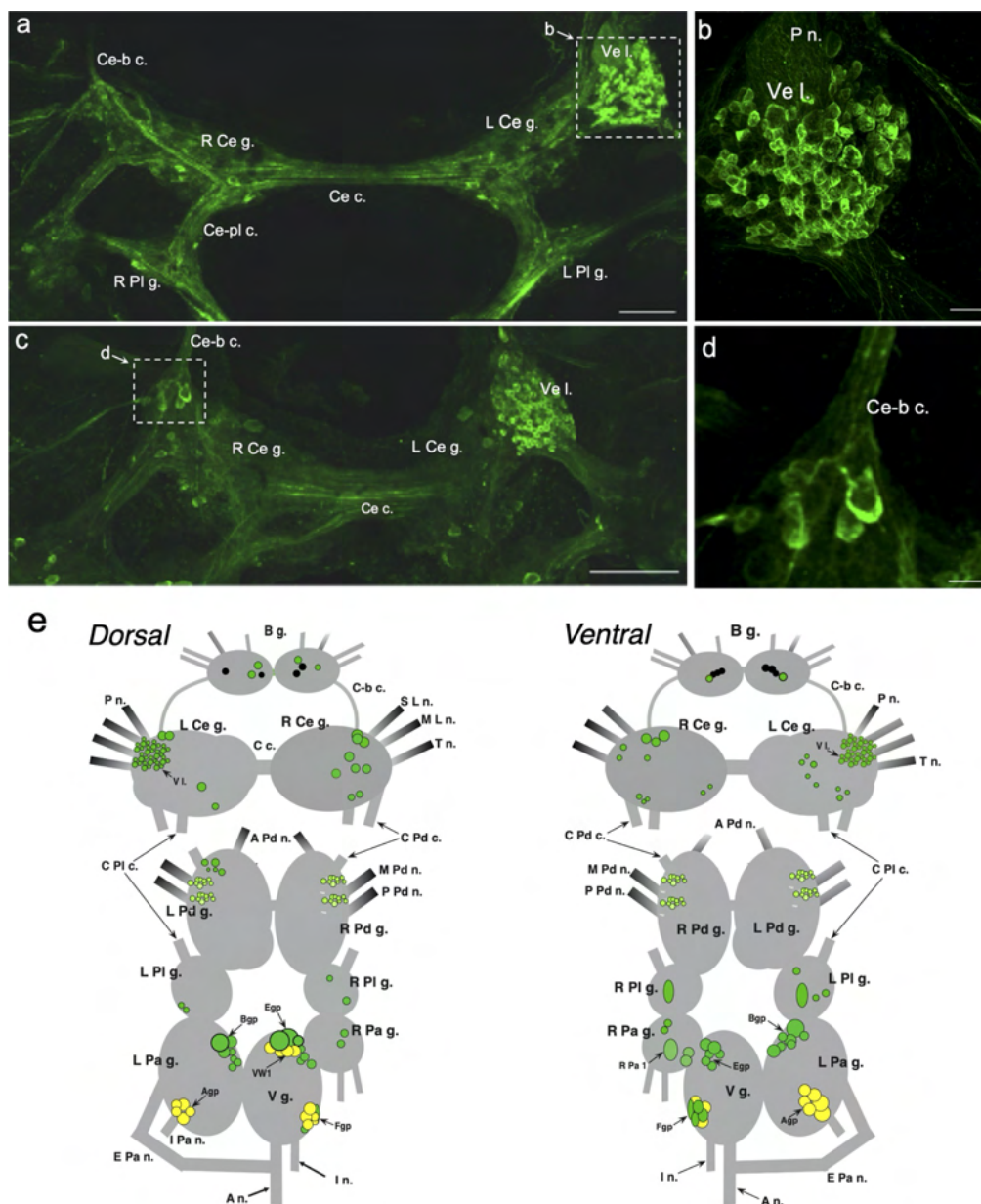


**FIGURE 2** FMRF-NH<sub>2</sub>-like immunoreactivity in *Biomphalaria* snails. (a) FMRF-NH<sub>2</sub>-li in the cerebral ganglia of *B. glabrata* (ventral surface shown). Most of the labeled cells were located in the ventral lobe (V l.; dashed square). Calibration bar = 100  $\mu$ m. (b) Ventral lobe of *B. glabrata* shown at higher magnification. The V l. is located at the origin of the penis nerve (P n.). Calibration bar = 30  $\mu$ m. (c) FMRF-NH<sub>2</sub>-li in the paired cerebral ganglia of *B. alexandrina* (ventral surface shown). Intensely staining cells were present at the base of the cerebral-buccal connective (dotted square). Calibration bar = 200  $\mu$ m. (d) Higher magnification of region enclosed by the dotted rectangle in panel (c). Calibration bar = 30  $\mu$ m. (e) Schematic summary of FMRF-NH<sub>2</sub>-related peptide (FaRP) localization in the CNS of *Biomphalaria* snails. Cells expressing the tetrapeptide *Bgl*-FaRP1 precursor are shown in green and neurons expressing the heptapeptide *Bgl*-FaRP2/3 precursor are colored yellow [Color figure can be viewed at [wileyonlinelibrary.com](http://wileyonlinelibrary.com)]

retrograde labeling were combined with immunohistochemistry for FMRF-NH<sub>2</sub>-like immunoreactivity and the SEEPTY peptide supported our previous finding that the majority of FaRP neurons in the ventral lobe do not project to the penis nerve (Figure 4(d–f)). However, as with the FMRF-NH<sub>2</sub>-li experiments, a subset of the backfilled ventral lobe neurons was labeled by the *Bgl*-FaRP1 antibody (Figure 4(d–f), arrows). Together, these findings indicate that the majority of FMRF-NH<sub>2</sub>-li ventral lobe neurons do not project to the penis nerve, but those that do express the tetrapeptide precursor *Bgl*-FaRP1.

The presence of FMRF-NH<sub>2</sub>-li neurons in the ventral lobe that were not labeled with penis nerve backfills was indicative of heterogeneity among the cells comprising this cluster. The DNA marker DAPI was therefore used to estimate the number of cells comprising the ventral lobe (Figure 5). DAPI labeled  $218.3 \pm 17.8$  ( $n = 3$ ) nuclei in the lobe (Figure 5(b)), of which  $93.6 \pm 22.3$  ( $n = 3$ ) were in neurons labeled by the biocytin backfills (Figure 5(a,c)). Together with the double-labeling experiments described above (P n. backfill  $\times$  FMRF-NH<sub>2</sub>-li or SEEPTY-li), our observations suggest that more than half of



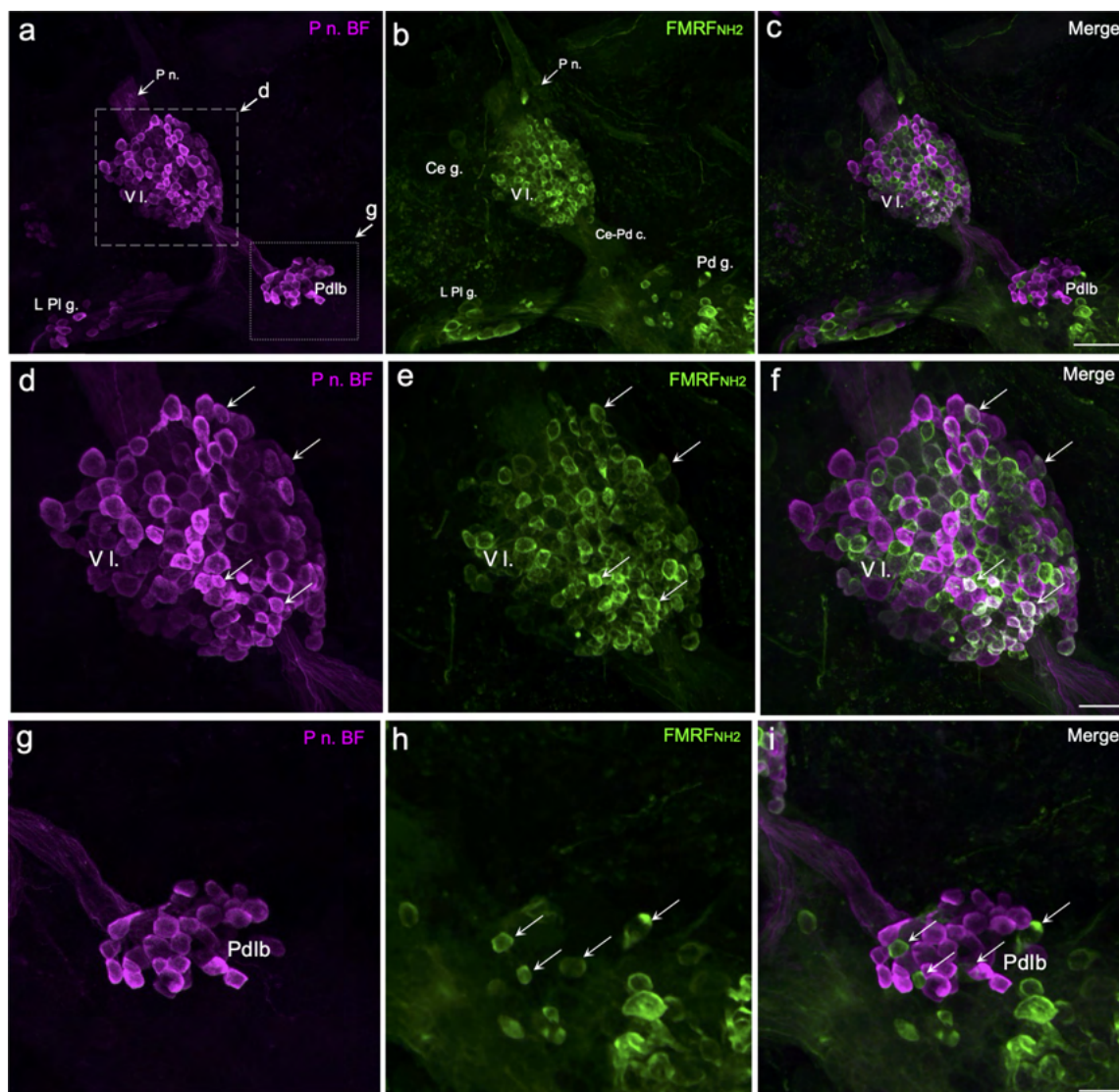


**FIGURE 3** FMRF-NH<sub>2</sub>-like immunoreactive penial nerve projections. (a) Biocytin backfill of the penial nerve (*P n.* BF) labeled cells in the ventral lobe (*V.I.*) of the left cerebral hemiganglion and a group of neurons in the *Pdlb* cluster of the left pedal hemiganglion (*Pe g.*). In this preparation, the pedal commissure was severed and the pedal hemiganglia were reflected to reveal their dorsal surface. (b) Whole-mount immunohistochemistry on the same preparation labeled FMRF-NH<sub>2</sub>-li neurons in the ventral lobe and in the region of the *Pdlb* cluster. *L. Pl g.*, left pleural ganglion; *Ce-Pd c.*, cerebral-pedal connective. (c) In an overlay of panels (a) and (b), double-labeled cells, (FMRF-NH<sub>2</sub>-li neurons that project to the penis nerve) appear white. Double-labeled cells are observed in the ventral lobe, but not in the pedal ganglion. Calibration bar = 100  $\mu$ m, applies to panels (a)–(c). (d) Higher magnification of the ventral lobe (area enclosed by dashed rectangle in panel a). (e) FMRF-NH<sub>2</sub>-li neurons in the ventral lobe. (f) Overlay of panels (d) and (e). The majority of backfilled cells (*magenta*) were not labeled with FMRF-NH<sub>2</sub> immunohistochemistry (*green*) and the majority of the FMRF-NH<sub>2</sub>-li neurons were not labeled by the backfill. However, some backfilled neurons also exhibited FMRF-NH<sub>2</sub>-like immunoreactivity (*white*, four indicated by arrows). Calibration bar = 30  $\mu$ m, applies to panels (d)–(f). (g) Higher magnification of the *Pdlb* region of the left pedal ganglion (area enclosed by dotted rectangle in panel a). (h) FMRF-NH<sub>2</sub>-li neurons (*green*) in the region of the *Pdlb* cluster. (i) Overlay of panels (g) and (h). None of the FMRF-NH<sub>2</sub>-li cells (four shown with arrows) were labeled by the penis nerve backfill. Calibration bar = 30  $\mu$ m, applies to panels (g)–(i) [Color figure can be viewed at [wileyonlinelibrary.com](http://wileyonlinelibrary.com)]

the ventral lobe neurons, including >80% of the FMRF-NH<sub>2</sub>-li neurons in the cluster, do not project to the penial nerve (see Section 4).

Projections to the penial nerve from the left pleural and parietal ganglia were also examined, as the innervation of male reproductive structures by FaRP heptapeptides originates from pleural and parietal neurons in *L. stagnalis* (El Filali et al., 2015; van Golen et al., 1995). Backfills of the penis nerve labeled approximately 20 cells dispersed

throughout the left pleural ganglion (Figure 6(a,d)). In double-labeling experiments, none of the left pleural ganglion cells labeled by penis nerve backfills exhibited FMRF-NH<sub>2</sub>-like immunoreactivity (Figure 6(a–f)). Penis nerve backfills also labeled two clusters of small (10–20  $\mu$ m) cells in the left parietal ganglion (Figure 6(g)). Again, no instances of double labeling were detected when retrograde fills were compared with FMRF-NH<sub>2</sub> immunohistochemistry (Figure 6(h,i)).



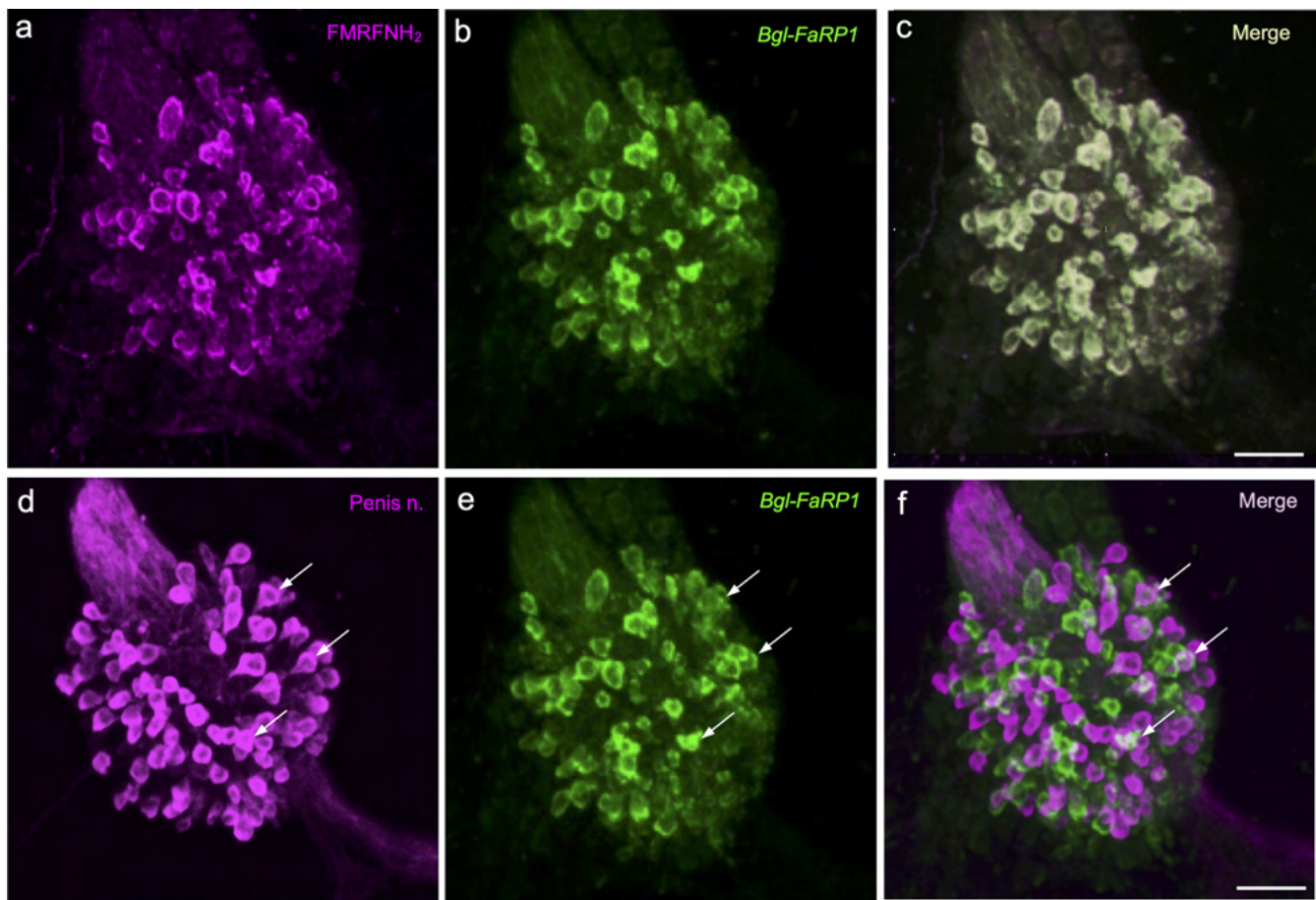


**FIGURE 4** The FMRF-NH<sub>2</sub>-like immunoreactive neurons in the ventral lobe are labeled by an antibody specific for the *Bgl-FaRP1* tetrapeptide precursor. (a) FMRF-NH<sub>2</sub>-li neurons in the ventral lobe of *B. glabrata* viewed with an Alexa 546 conjugate (magenta pseudo-color). (b) The same preparation was processed with a goat antibody against the SEEPTY peptide of the *Bgl-FaRP1* (see Figure 1) and visualized with an Alexa 488 second antibody (green). (c) Overlay of panels (a) and (b) showed that all of the FMRF-NH<sub>2</sub>-li neurons in the ventral lobe were also labeled with the SEEPTY antibody (white). Calibration bar = 50  $\mu$ m applies to panels (a)–(c). (d) Ventral lobe neurons labeled by penis nerve backfill with biocytin and visualized with streptavidin Pacific blue conjugate (magenta pseudo-color). Same preparation as panel (a). (e) SEEPTY-like immunoreactivity visualized with an Alexa 488 conjugate second antibody (green). (f) Overlay of panels (d) and (e) shows double labeling in dispersed V I. cells (arrows), as observed with the FMRF-NH<sub>2</sub> antibody (Figure 3(d–f)). Calibration bar = 50  $\mu$ m, applies to panels (d)–(f) [Color figure can be viewed at [wileyonlinelibrary.com](http://wileyonlinelibrary.com)]

### 3.4.2 | Feeding

Consummatory feeding behaviors of gastropods are largely controlled by circuits of the buccal and cerebral ganglia (Elliott & Susswein, 2002; Kupfermann, 1974; Murphy, 2001). FMRF-NH<sub>2</sub>-li cells were present on the ventral surface of the buccal ganglia (Figure 7(a–i); Figure 8(a–c), (g–i)). A symmetrical group of four to five moderately sized (15–30  $\mu$ m) FMRF-NH<sub>2</sub>-li cells spanned the medial region of each hemiganglion (Figure 7(a)). In double-labeling experiments, the largest and most lateral member of each FMRF-NH<sub>2</sub>-li cluster was also labeled by antibodies specific for the *Bgl-FaRP1* tetrapeptide precursor (Figure 7(a–i)). No buccal neurons were detected by the *Bgl-FaRP2/3* heptapeptide precursor antibodies (not shown).

Integration between the buccal and cerebral ganglia of gastropods is achieved by cerebral-buccal interneurons (CBIs) and buccal-cerebral

interneurons (BCIs; Gillette et al., 1978; McCrohan & Croll, 1997; Rosen et al., 1991). As CBIs tend to be concentrated in the anterolateral quadrant of the cerebral ganglia, where several FMRF-NH<sub>2</sub>-li neurons were located (Figure 2(c,d)), double-labeling experiments were conducted combining retrograde labeling of the cerebral-buccal connectives (C-b c.) with FMRF-NH<sub>2</sub>-like immunoreactivity (Figure 8). Double labeling was observed in one ipsilateral cell near the origin of the C-b c. (Figure 8(d–f)), indicating the presence of FaRPs in a CBI.

Some backfills of the cerebral-buccal connectives toward the cerebral ganglia were performed with the buccal ganglia connected via the contralateral C-b c. (Figure 8). The majority of buccal neurons labeled by a biocytin backfill of the right C-b c. were located in the right buccal hemiganglion (Figure 8(a,g)), suggesting that axons of these cells project through the entire cerebral-buccal loop to return to their ganglion of origin. FMRF-NH<sub>2</sub>-li labeling was observed in two such neurons in the right buccal hemiganglion (Figure 8(g–i)).

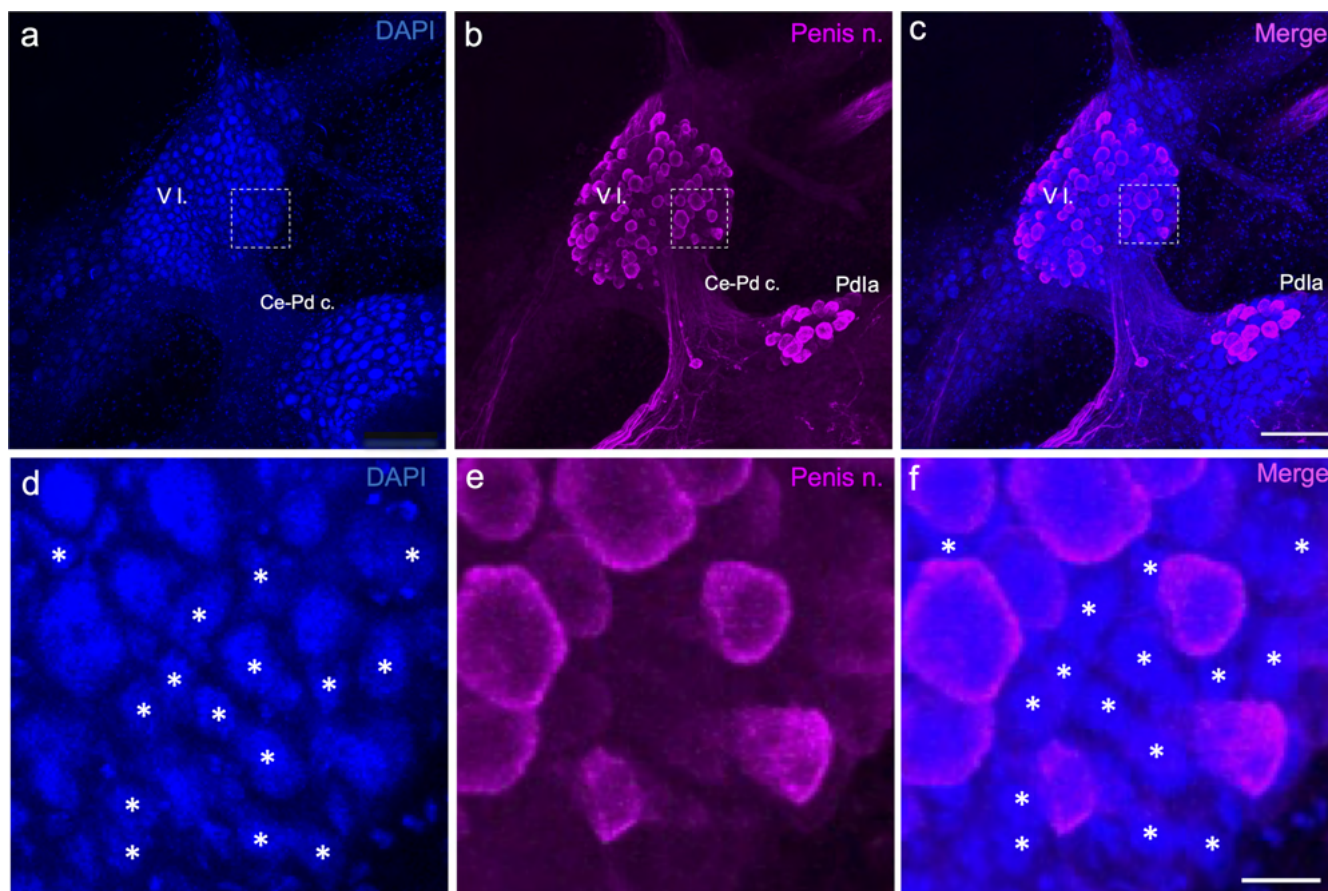


**FIGURE 5** The majority of ventral lobe neurons do not project to the penis nerve. (a) DAPI nuclear staining enabled an estimation of the number of cells comprising the ventral lobe (V.I.) of *B. glabrata*. (b) Neurons labeled by backfill of the penis nerve of *B. glabrata*. Same preparation as (a). (c) Overlay of panels (a) and (b) demonstrates the presence of nuclei throughout the V.I. that do not correspond to neurons labeled by the backfill. Calibration bar = 100  $\mu$ m, applies to panels (a)–(c). (d) Higher magnification of V.I. region enclosed by dashed rectangle in panel (a). Asterisks mark nuclei of cells that were not labeled by the backfill. (e) Backfilled neurons in region enclosed by rectangle in (b). (f) Overlay of panels (d) and (e). Calibration bar = 10  $\mu$ m, applies to panels (d)–(f) [Color figure can be viewed at [wileyonlinelibrary.com](http://wileyonlinelibrary.com)]

In *L. stagnalis* and *Helisoma trivolvis*, the buccal feeding circuit is inhibited by a FMRF-NH<sub>2</sub>-li neuron that projects from the pleural ganglia (Alania et al., 2004; Murphy, 1990). A prominent FMRF-NH<sub>2</sub>-li cell was located in each pleural ganglion of *Biomphalaria* spp. (Figure 9(a)). Double-labeling experiments localized the *Bgl-FaRP1* tetrapeptide precursor to this cell (Figure 9(b,c)). However, projections from the pleural ganglia were not detected with retrograde labeling of the cerebral-buccal connective (e.g., Figure 8, see Section 4).

### 3.4.3 | Cardiorespiratory system

In pulmonates, central control of cardiac and respiratory function originates from the parietal and visceral ganglia (Chase, 2002; Syed & Winlow, 1991). Four to six FMRF-NH<sub>2</sub>-li neurons were labeled in the right parietal ganglion, including one giant cell (80–100  $\mu$ m) near the ventral surface (Figure 9(d)). The right parietal FMRF-NH<sub>2</sub>-li neurons were labeled with the *Bgl-FaRP1* specific antibody (Figure 9(e,f)). Staining with both antibodies was weaker than in other ganglia, suggesting a lower level of FaRP expression. This finding agreed with

observations in the dextral snail *L. stagnalis*, where low levels of FaRP immunoreactivity were observed in the giant LP1 neuron in the left parietal ganglion (Bright et al., 1993; Santama et al., 1993). The giant FMRF-NH<sub>2</sub>-li neuron in the right parietal ganglion of *Biomphalaria* spp., a sinistral snail, was thus designated RPa1 (Figure 9(d–f)).

On the dorsal surface of the left parietal ganglion, prominent FMRF-NH<sub>2</sub>-li labeling was observed in an anteromedial cluster of large neurons (Figure 10(a,e); see also Figure 6(g–i)). The strongest immunoreactivity occurred in the largest and most anterior neuron, with a decreasing gradient of intensity in the cells extending in the posterior direction. All of the FMRF-NH<sub>2</sub>-li cells in this cluster were labeled with the *Bgl-FaRP1* specific antibody (Figure 10(b,f)). The anterior to posterior gradient in labeling intensity was also observed with mRNA labeling by a probe specific for the *Bgl-FaRP1* transcript (Figure 10(d,h)). The location and staining pattern of this cluster corresponds to the B group (Bgp) of neurons in the right parietal ganglion of *L. stagnalis* (Benjamin & Winlow, 1981; Bright et al., 1993).

The B group extended around to the ventral side of the left parietal ganglion, where strong FMRF-NH<sub>2</sub>-li labeling was present in a second large anterior cell (Figure 11(a,d)). *In situ* hybridization with the *Bgl-FaRP1*



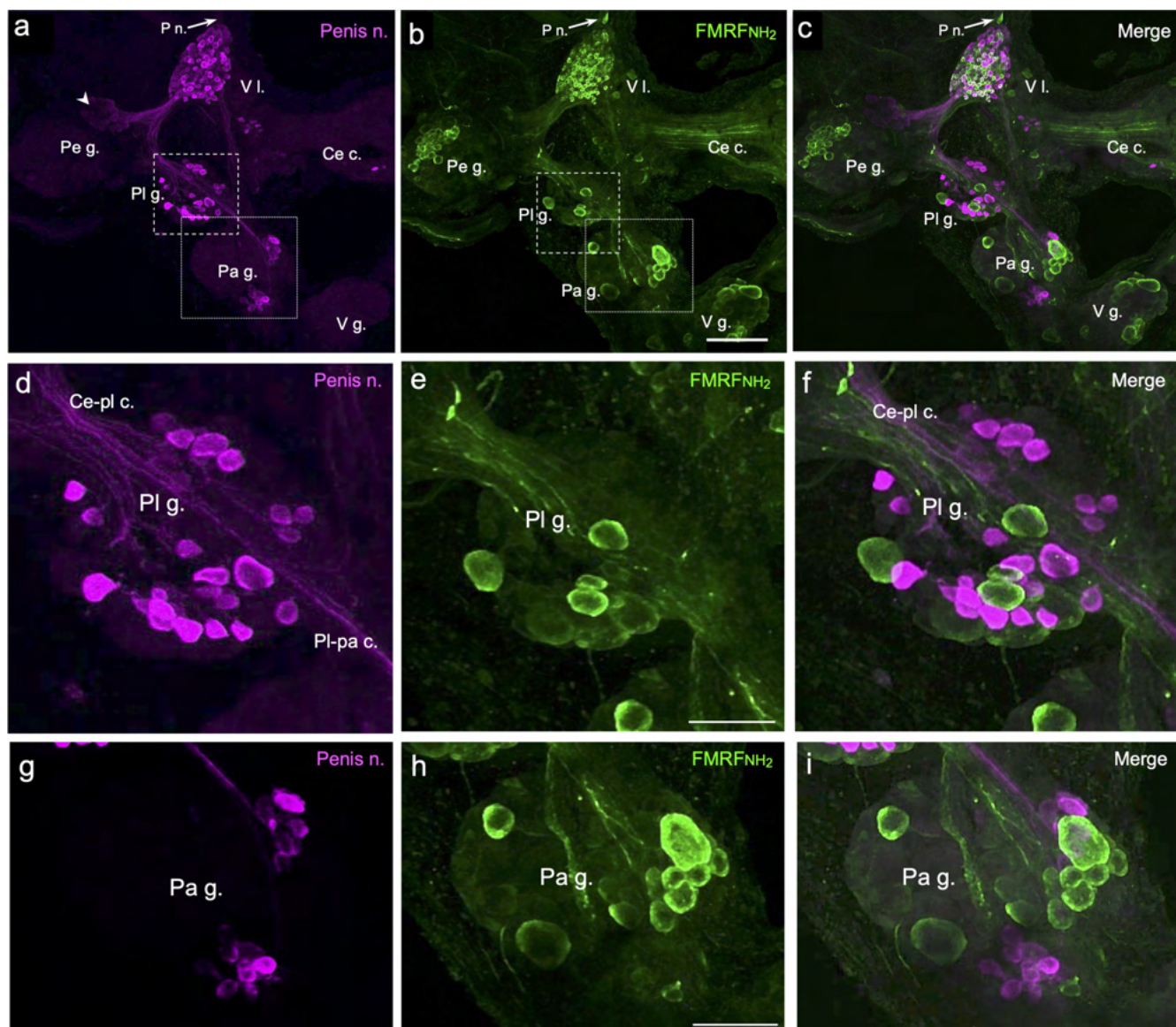


**FIGURE 6** Projections to the penial nerve from the left pleural and parietal ganglia. (a) Backfill of the penial nerve (*P n.*) of *B. alexandrina* labeled neurons (magenta) in the ventral lobe (*V l.*) of the cerebral ganglion, dispersed cells throughout the pleural ganglion (*Pl g.*), and two clusters of neurons in the left parietal ganglion (*Pa g.*). Arrowhead: The *Pdlb* cluster of neurons, which lies on the dorsal surface of the pedal ganglion (Figure 3(a,g)), is weakly visible from this ventral perspective. *Ce c.*, cerebral commissure; *Pe g.*, pedal ganglia; *V g.*, visceral ganglion. (b) The backfilled preparation in (a) was processed for FMRF-NH<sub>2</sub>-like immunoreactivity (green). Calibration bar = 200  $\mu$ m, applies to panels (a)–(c). (c) In an overlay of panels (a) and (b), no FMRF-NH<sub>2</sub>-li projections to the *P n.* were detected from either the pleural or parietal ganglion. (d) Enlargement of the left pleural ganglion; region enclosed by dashed rectangle in (a). (e) FMRF-NH<sub>2</sub>-like immunoreactivity in the pleural ganglion; region enclosed by dashed rectangle in (b). Calibration bar = 100  $\mu$ m, applies to panels (d)–(f). (f) In an overlay of panels (d) and (e), no double-labeled neurons were observed. (g) Enlargement of the left parietal ganglion; region enclosed by dotted rectangle in (a). (h) FMRF-NH<sub>2</sub>-like immunoreactivity in the left parietal ganglion; region enclosed by dotted rectangle in (b). Calibration bar = 100  $\mu$ m, applies to panels (g)–(i). (i) In an overlay of panels (g) and (h), no double-labeled neurons were detected in the parietal ganglion [Color figure can be viewed at [wileyonlinelibrary.com](http://wileyonlinelibrary.com)]

probe also produced intense labeling of the large ventral Bgp cell (Figure 11(e)). No cells in the ventral Bgp were labeled by the antibody specific for the *Bgl-FarP2/3* precursor (Figure 11(b,c)). The *Bgl-FarP2/3* antibody did label a cluster of FMRF-NH<sub>2</sub>-li neurons in the posterior region of the ventral left parietal ganglion (Figure 11(b,c,f)), supporting its utility for identifying neurons that express the

heptapeptide precursors. The posterior FMRF-NH<sub>2</sub>-li cluster was assigned to the A group (Agp) of parietal neurons following the nomenclature established in *L. stagnalis* (Figure 11(a–c); see Benjamin & Winlow, 1981).

In the visceral ganglion, an anterior cluster of FMRF-NH<sub>2</sub>-li neurons was located near the right parietal-visceral connective



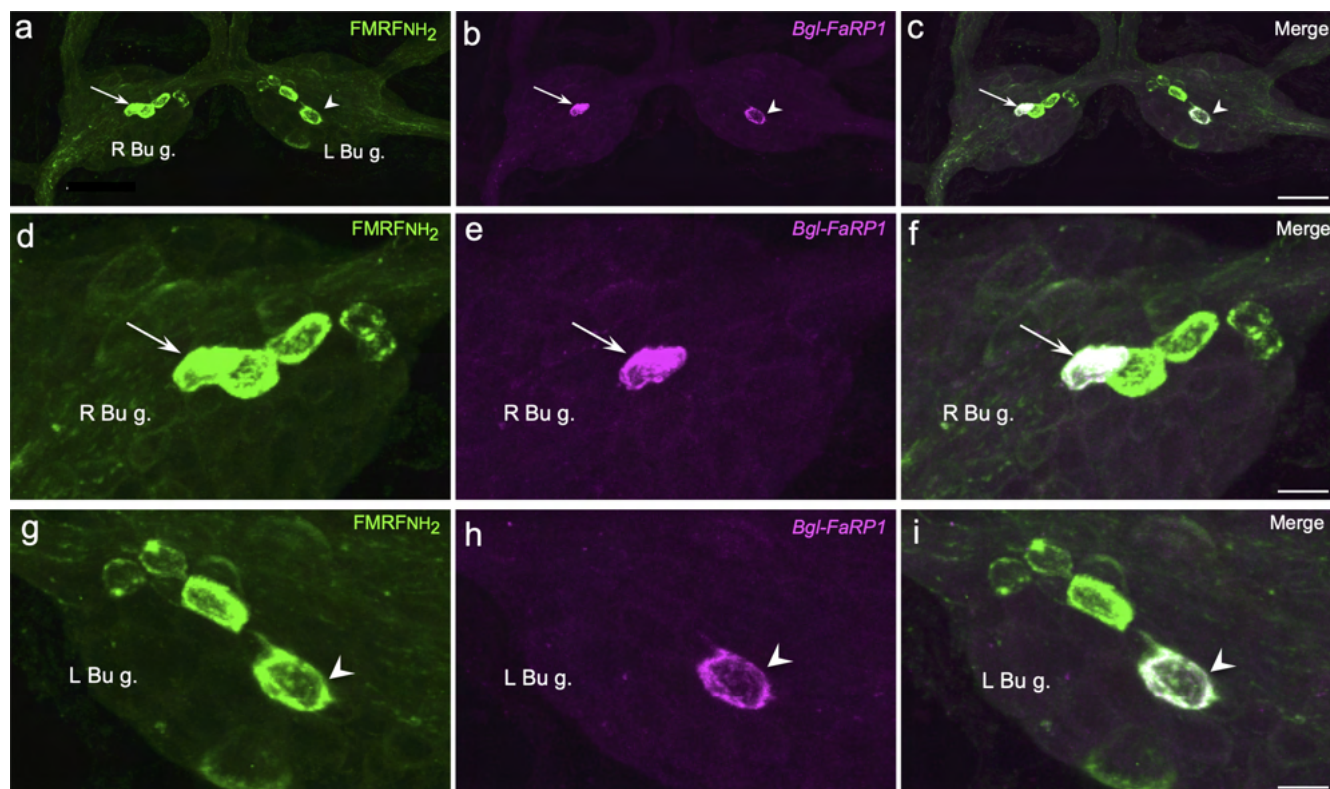


**FIGURE 7** FMRF-NH<sub>2</sub>-like immunoreactive neurons on the ventral surface of the buccal ganglia. (a) FMRF-NH<sub>2</sub>-like immunoreactive neurons (green) on the ventral surface of the paired buccal ganglia of *B. glabrata*. (b) The same preparation as (a) was processed with the SEEPTY antibody specific for the *Bgl-FaRP1* precursor. One neuron (magenta) was labeled in the right (arrow) and left (arrowhead) buccal ganglia. (c) Overlay of panels (a) and (b) shows that the neuron labeled with the *Bgl-FaRP1* antibody corresponds to the most lateral FMRF-NH<sub>2</sub>-li cell in each hemiganglion (white, arrow, arrowhead). Calibration bar = 100  $\mu$ m, applies to (a)–(c). (d) Higher magnification of FMRF-NH<sub>2</sub>-li neurons in the right buccal hemiganglion (R Bu g.). (e) Same field as (d) showing single cell labeled by the *Bgl-FaRP1* antibody. (f) Overlay of panels (d) and (e) confirms double-labeling of the most lateral FMRF-NH<sub>2</sub>-li neuron. Calibration bar = 30  $\mu$ m, applies to panels (d)–(f). (g) Higher magnification of FMRF-NH<sub>2</sub>-li neurons in the left buccal hemiganglion (L Bu g.). (h) Same field as (g) showing single cell labeled by the *Bgl-FaRP1* antibody. (i) Overlay of panels (g) and (h) confirms double-labeling of the most lateral FMRF-NH<sub>2</sub>-li neuron in the left buccal hemiganglion. Calibration bar = 30  $\mu$ m, applies to panels (g)–(i) [Color figure can be viewed at [wileyonlinelibrary.com](http://wileyonlinelibrary.com)]

(Figure 12(a)). Most of the dorsal cells comprising this cluster, designated the E group (Egp), were also labeled by the *Bgl-FaRP1* antibody (Figure 12(a–c)). The two most anterior Egp neurons were larger than the other members of the cluster (Figure 12(a–c), asterisks). When the visceral ganglion was labeled with a specific probe for the *Bgl-FaRP1* transcript, the two large anterior cells exhibited high expression levels (Figure 12(d), asterisks).

The strongest labeling by the *Bgl-FaRP2/3* heptapeptide antibody in the visceral ganglion occurred in a posterolateral cluster of cells that corresponds to the F group (Fgp) described in *L. stagnalis* (Figure 12(e–h); Benjamin & Winlow, 1981; Bright et al., 1993; Santama et al., 1993). The *Bgl-FaRP2/3* antibody also produced weaker labeling of six to eight medium sized (40–60  $\mu$ m) cells in the E group (Figure 12(j,k)). In *L. stagnalis*, signaling by the FMRF-NH<sub>2</sub>-related heptapeptides originates from the Egp visceral white interneuron (VWI), a key element of the cardiorespiratory central pattern generator network (Buckett, Peters, & Benjamin, 1990; Buckett, Peters, Dockray, et al., 1990; Skingsley et al., 1993; see Section 4).

In *Biomphalaria* spp., the extrinsic parietal nerve courses in the posterior direction and merges with the anal nerve (Lever et al., 1965;

Vallejo et al., 2014). The fused nerves enter the body wall, innervating the anus and pneumostome, among other organs (Lever et al., 1965). Retrograde tracing of the anal nerve labeled a cluster of cells in the Fgp (Figure 12(i)). Subsequent immunohistochemistry with the *Bgl-FaRP2/3* antibody labeled three or four of the Fgp neurons that project to the anal nerve (Figure 12(j–l)). Notably, not all backfilled neurons in the Fgp were FMRF-NH<sub>2</sub>-li and not all FMRF-NH<sub>2</sub>-li neurons were backfilled. Together, these observations indicate that FaRPs derived from both tetrapeptide and heptapeptide precursors participate in control of the cardiorespiratory system of *Biomphalaria* spp. (see Section 4).

## 4 | DISCUSSION

This study supports the participation of FaRPs in diverse physiological and behavioral systems of *Biomphalaria* species. The precursor organization and the localization of this neuropeptide system share many features with other gastropods, especially the thoroughly characterized FaRP family of *L. stagnalis* (reviewed by Benjamin & Burke, 1994;

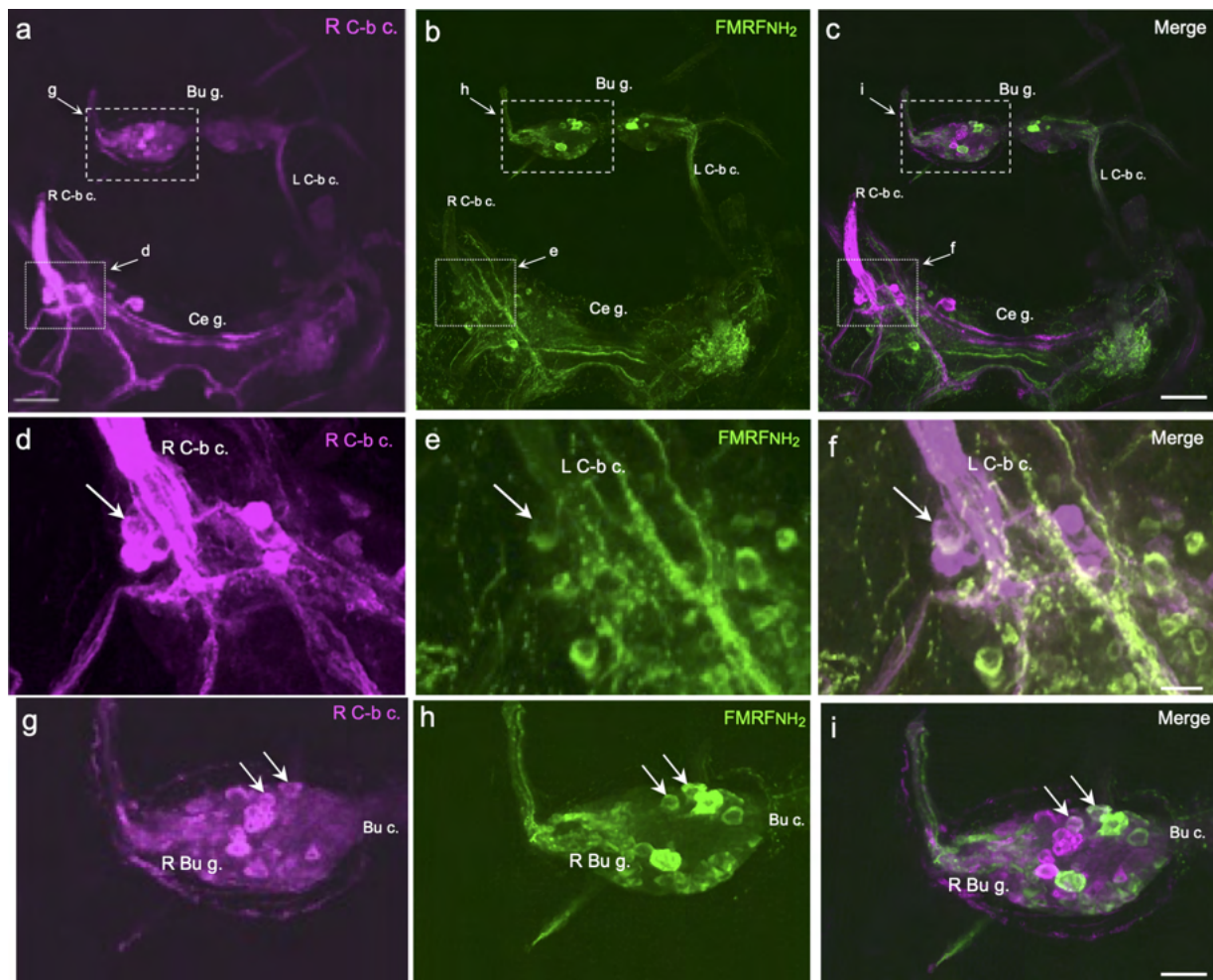


**FIGURE 8** FMRF-NH<sub>2</sub>-li projection neurons in the feeding system of *Biomphalaria glabrata*. (a) A biocytin backfill of the left cerebral-buccal connective (L C-b c.) toward the cerebral ganglion labeled several cerebral-buccal interneurons (CBIs) in the anterolateral quadrant of the ganglion (dotted rectangle, dorsal surface shown). The C-b c. backfill also labeled several smaller buccal-cerebral interneurons (BCIs) in the left buccal ganglion (dashed rectangle). (b) Same preparation as (a) processed for FMRF-NH<sub>2</sub>-like immunoreactivity (green). (c) Overlay of panels (a) and (b). CBIs and BCIs that express FMRF-NH<sub>2</sub>-like immunoreactivity appear white. Calibration bar = 100  $\mu$ m, applies to panels (a)–(c). (d) Enlargement of region enclosed by dotted rectangle in panel (a). (e) Enlargement of region enclosed by dotted rectangle in panel (b). One FMRF-NH<sub>2</sub>-li CBI near the origin of the C-b c. was labeled (compare arrows in panels (d) and (e)). (f) Overlay of panels (d) and (e) confirms co-labeling of one FMRF-NH<sub>2</sub>-li neuron by the C-b c. backfill (arrow). Calibration bar = 30  $\mu$ m, applies to panels (d)–(f). (g) Enlargement of region enclosed by dashed rectangle in panel (a). (h) Region enclosed by dashed rectangle in panel (b). Two FMRF-NH<sub>2</sub>-li BCIs in the anterior region of left buccal ganglion (arrows) were labeled (compare arrows in panels (g) and (h)). (i) Overlay of panels (g) and (h) confirms co-labeling of two FMRF-NH<sub>2</sub>-li neurons by the backfill of the left C-b c. (arrows). Calibration bar = 20  $\mu$ m, applies to panels (g)–(i) [Color figure can be viewed at [wileyonlinelibrary.com](http://wileyonlinelibrary.com)]

Santama & Benjamin, 2000). Our findings suggest, however, that the *Biomphalaria* FMRF-NH<sub>2</sub> neuropeptide system exhibits some distinguishing properties that could impact its role in the regulation of neural circuits and behavior.

#### 4.1 | The *Biomphalaria* FaRP transcripts and precursors

Alternative splicing is broadly used to generate distinct FaRP transcripts in gastropods (Cummins et al., 2011; Lutz et al., 1992; Santama & Benjamin, 2000; Saunders et al., 1991). In *Biomphalaria*, as

in the pulmonates *L. stagnalis* and *H. aspersa*, a common 5' exon that includes the signal sequence (termed Exon I in *Lymnaea*) is alternatively spliced to a tetrapeptide-encoding (Exon II) or a heptapeptide-encoding exon (Exon III). Unlike the other species, however, our results suggest an additional locus of alternative splicing that can generate two distinct heptapeptide precursors. In *L. stagnalis*, the heptapeptide precursor is encoded by four exons (I, III, IV, and V) with the splice junction between the last two exons located within the sequence encoding SKPYMRF-NH<sub>2</sub> (Kellett et al., 1994). Our *B. glabrata* transcriptome disclosed two heptapeptide transcripts, one that completed the sequence for SKPYMRF-NH<sub>2</sub> (*Bgl-FaRP2*) and one that did not (*Bgl-FaRP3*). If the splicing patterns of the genomic



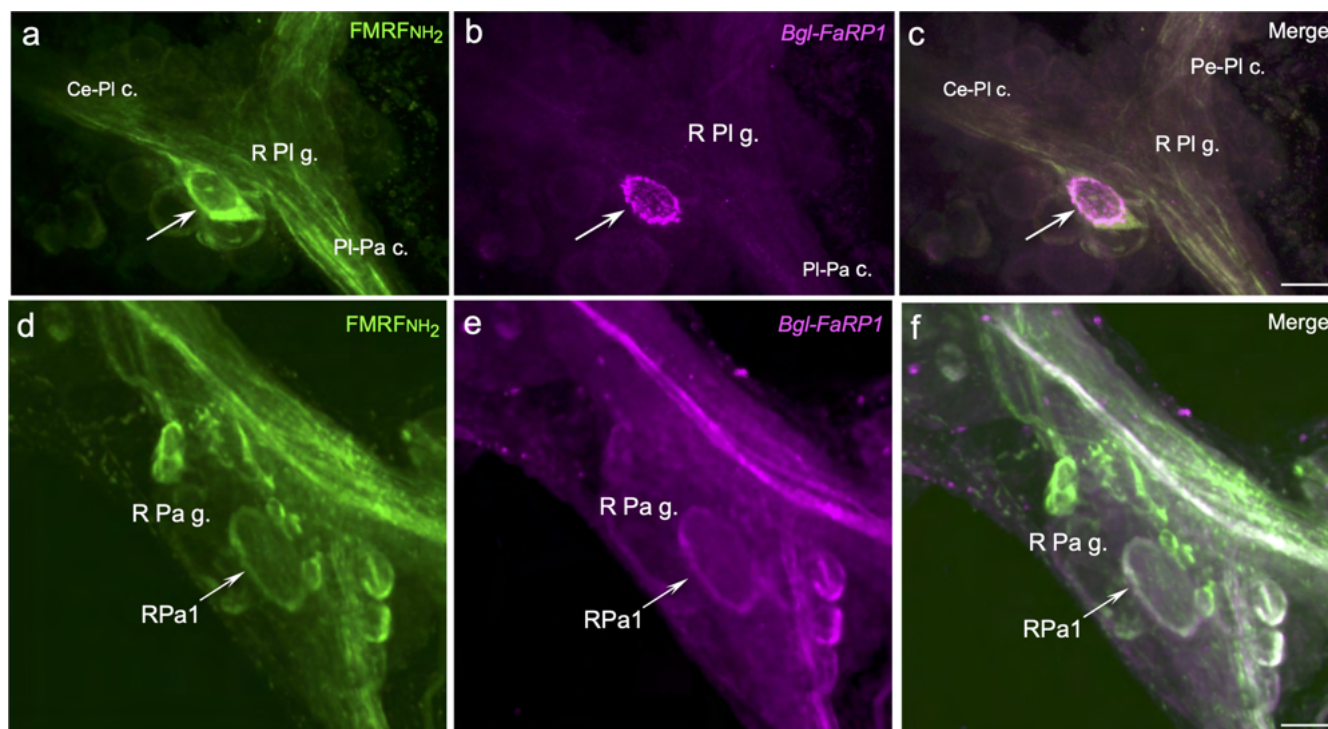


**FIGURE 9** FMRF-NH<sub>2</sub>-li neurons in the right pleural and parietal ganglia of *Biomphalaria glabrata*. (a) A single FMRF-NH<sub>2</sub>-li neuron (arrow) was located on the ventral surface of the right pleural ganglion of *B. glabrata*. (b) The same cell was labeled by an antibody specific for the *Bgl-FaRP1* precursor. (c) Overlay of panels (a) and (b) demonstrates colocalization of FMRF-NH<sub>2</sub>-like immunoreactivity and labeling by the *Bgl-FaRP1* antibody. Calibration bar = 50 μm, applies to panels (a–c). (d) FMRF-NH<sub>2</sub>-li neurons in the right parietal ganglion included a giant cell, designated *RPa1*. FMRF-NH<sub>2</sub>-like immunoreactivity in the right parietal ganglion was weaker than in other ganglia (compare panels (d) and (a)). (e) The *Bgl-FaRP1* antibody labeled all FMRF-NH<sub>2</sub>-li cells in the right parietal ganglion. *Bgl-FaRP1* labeling in the parietal ganglion was also less intense than in other ganglia (compare panels (b) and (e)). (f) Overlay of panels (d) and (e) demonstrates colocalization of FMRF-NH<sub>2</sub>-like immunoreactivity and *Bgl-FaRP1* in all but two small cells in the right parietal ganglion. Calibration bar = 50 μm, applies to panels (d–f) [Color figure can be viewed at [wileyonlinelibrary.com](http://wileyonlinelibrary.com)]

loci encoding the FaRP precursors of *Lymnaea* and *Biomphalaria* are otherwise conserved, our findings suggest that the *B. glabrata* gene consists of at least six exons and five introns.

All gastropod FaRP precursors described to date possess tetrabasic consensus cleavage signals for furin-like enzymes (Ahn et al., 2017; Cummins et al., 2011; Senatore et al., 2015; Taussig & Scheller, 1986). Such cleavage in the *trans* Golgi could enable differential sorting of the N-terminal and C-terminal peptides into distinct secretory vesicles, as observed in the hormone precursors that control ovulation in gastropods (Li et al., 1994; Sossin et al., 1990; Sweet-Cordero et al., 1990). The peptides located between the signal peptide and the tetrapeptide cleavage site of *Bgl-FaRP1* (two copies of FLRF-NH<sub>2</sub> and one pQFYRI-NH<sub>2</sub>) were identical to those found in the tetrapeptide precursor of *L. stagnalis* (Linacre et al., 1990). The number of copies of FMRF-NH<sub>2</sub> following the tetrabasic site, however, is highly variable among the gastropods with 8 present in *B. glabrata*, 9 in *L. stagnalis* (Linacre et al., 1990), 16 in the slug *Deroceras reticulatum* (Ahn et al., 2017), and 28 in *A. californica* (Taussig & Scheller, 1986).

Precursors for extended FaRPs have been identified in some, but not all, gastropod groups (see Cummins et al., 2011; Vilim

et al., 2010). In the *Bgl-FaRP2* and *Bgl-FaRP3* precursors, the heptapeptide GDPFLRF-NH<sub>2</sub> was present in 14 copies between the signal peptide and the tetrapeptide cleavage site (Figure 1(a,b)). In other gastropods, the heptapeptide complement is more heterogeneous. The heptapeptide precursor of *L. stagnalis* includes seven copies of GDPFLRF-NH<sub>2</sub> and six copies of SDPFLRF-NH<sub>2</sub> (Saunders et al., 1991) and the corresponding precursor of *D. reticulatum* contains a total of nine copies of six distinct heptapeptides (Ahn et al., 2017). In early biochemical studies, GDPFLRF-NH<sub>2</sub> was the only heptapeptide purified from the nervous system of *H. trivolvis* (Bullock et al., 1988). Considered together with the present observations, homogeneity of the heptapeptide complement may be a unique property of the planorbid snail group.

In *L. stagnalis*, two long non-FaRP peptides are expressed as steady-state final products of the FaRP precursors (Santama et al., 1993, 1996). These peptides, termed “SEEPLY” in the tetrapeptide precursor and “acidic peptide” in the heptapeptide precursor, are both flanked at their carboxyl terminus by the furin-like cleavage site of their respective precursors (Santama & Benjamin, 2000). In this study, the antibodies utilized to localize the *Bgl-FaRP1* and *Bgl-FaRP2/3* were generated against sequences within



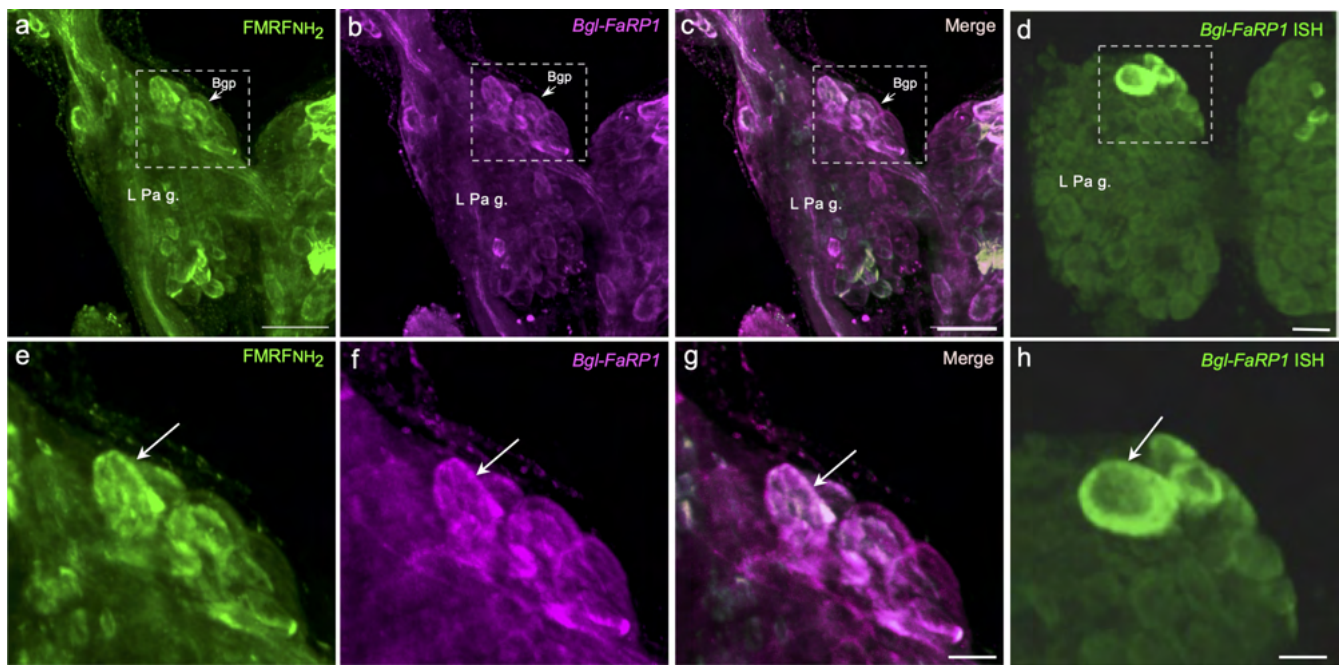


**FIGURE 10** FMRF-NH<sub>2</sub>-like immunoreactivity on the dorsal surface of the left parietal ganglion. (a) An anteromedial cluster of FMRF-NH<sub>2</sub>-li cells, designated the B group (Bgp), was located on the dorsal surface of the *B. glabrata* left parietal ganglion. (b) Double labeling showed that the Bgp neurons expressed the *Bgl-FaRP1* precursor. (c) Overlay of panels (a) and (b) confirmed that the FMRF-NH<sub>2</sub>-li cells in the Bgp express the *Bgl-FaRP1* precursor. Calibration bar = 100  $\mu$ m, applies to panels (a–c). (d) In situ hybridization detected the *Bgl-FaRP1* transcript in the Bgp cells. Calibration bar = 50  $\mu$ m. (e) Enlargement of the Bgp (area enclosed by dashed rectangle in (a)) showed that the most anterior Bgp neuron (arrow) was the largest and most intensely labeled cell in the group. (f) The *Bgl-FaRP1* antibody also produced an anterior-to-posterior gradient in labeling intensity (arrow). (g) Overlay of panels (e) and (f) confirmed that the more posterior cells exhibited less intense labeling. Calibration bar = 30  $\mu$ m, applies to panels (e)–(g). (h) In situ hybridization verified the anterior-to-posterior gradient of *Bgl-FaRP1* expression in the Bgp. Calibration bar = 30  $\mu$ m [Color figure can be viewed at [wileyonlinelibrary.com](http://wileyonlinelibrary.com)]

the “SEEPTY” peptide (*Bgl-FaRP1*) and “acidic peptide” (*Bgl-FaRP2/3*) that would result from similar posttranslational processing of the *B. glabrata* precursors. In both cases, labeling by the non-FaRP antibodies was observed in a subset of the neurons that exhibited FMRF-NH<sub>2</sub>-like immunoreactivity, suggesting that processing of the *Biomphalaria* precursors resembles that of *Lymnaea*. It was not possible to test the SEEPTY (goat) and acidic peptide (sheep) antibodies in double-labeling experiments, probably due to the evolutionary proximity of the two Caprinae hosts (see Section 2). Together, however, our double-labeling experiments using the FMRF-NH<sub>2</sub> antibody and each of the non-FaRP antibodies supports the mutually exclusive and -non-overlapping expression of the tetrapeptide precursor (*Bgl-FaRP1*) and the heptapeptide precursors (*Bgl-FaRP2/3*) as shown in *L. stagnalis* (Bright et al., 1993; Santama et al., 1995, 1996; Saunders et al., 1992) and *H. aspersa* (Cottrell et al., 1992; MacDonald et al., 1994). Whether such differential expression occurs between the two heptapeptide precursors, *Bgl-FaRP2* and *Bgl-FaRP3*, could be explored with in situ hybridization using transcript-specific probes (Santama et al., 1995).

## 4.2 | Male reproductive system

In gastropods, male mating behavior is controlled by a distributed central network located ipsilateral to the reproductive organs (de Boer

et al., 1996; Li & Chase, 1995; Van Duivenboden & Ter Maat, 1988). Numerous neuropeptides, including the FaRPs, have been localized to neurons that project to the male reproductive complex (de Lange, de Boer, et al., 1998; de Lange, Joosse, & van Minnen, 1998; Croll & Van Minnen, 1992; Smit et al., 2003; Acker et al., 2019; reviewed by Koene, 2010). The FMRF-NH<sub>2</sub> tetrapeptides and heptapeptides modulate contraction of the penis retractor muscle of *L. stagnalis* (van Golen et al., 1995), and addition of FMRF-NH<sub>2</sub> to the surrounding water causes penile eversion in *B. glabrata* (Fong et al., 2005; Muschamp & Fong, 2001).

Our finding that neurons in the ventral lobe express the tetrapeptide precursor agreed with prior observations in *L. stagnalis* (Bright et al., 1993; Santama et al., 1993; van Golen et al., 1995). The apparent abundance (>80%) of FMRF-NH<sub>2</sub>-li ventral lobe neurons that do not project directly to the penial nerve suggests additional roles for the tetrapeptides in the control and integration of mating behaviors (see de Lange, Joosse, & van Minnen, 1998; Li & Chase, 1995). Alternatively, this observation and others in which double-labeling were not observed (following text) could reflect incomplete labeling by the biocytin backfill method.

FMRF-NH<sub>2</sub>-li projections to the penial nerve were not detected from the pedal, pleural, or parietal ganglia (Figures 3 and 6). In *L. stagnalis*, innervation of the male reproductive system by the FaRP heptapeptides originates from neurons in the pleural

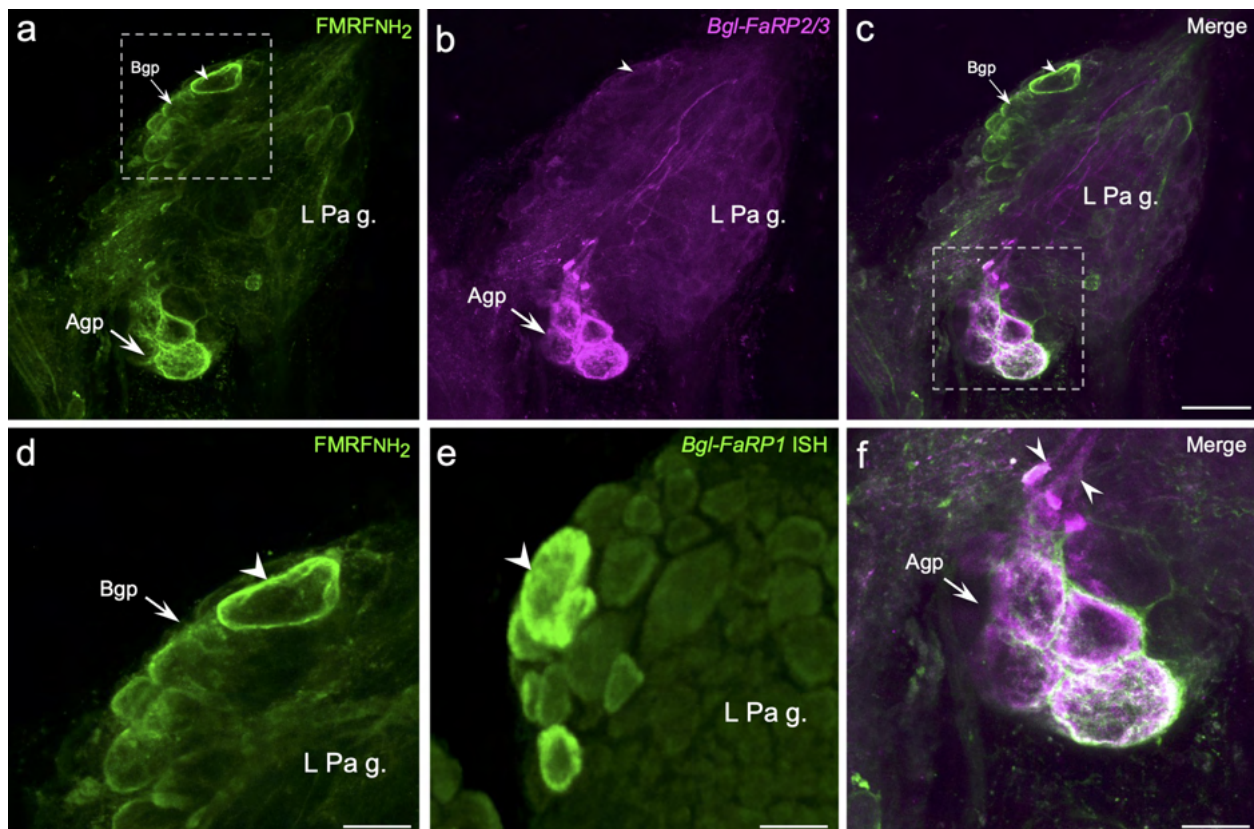


**FIGURE 11** FMRF-NH<sub>2</sub>-like immunoreactivity on the ventral surface of the left parietal ganglion. (a) The anteromedial Bgp cluster of FMRF-NH<sub>2</sub>-li cells, (see Figure 10a,e) extended around to the ventral surface of the *B. glabrata* left parietal ganglion. The most anterior ventral Bgp neuron (arrowhead) was larger (60–80 μm in length) and more intensely labeled than other members of the cluster. (b) The *Bgl-FaRP2/3* precursor-specific antibody did not label FMRF-NH<sub>2</sub>-li neurons in the Bgp. The *Bgl-FaRP2/3* antibody did label a group of cells at the posterior pole of the ganglion (magenta). (c) Overlay of panels (a) and (b) confirmed that four FMRF-NH<sub>2</sub>-li cells in the posterior cluster express the *Bgl-FaRP2/3* precursor. Calibration bar = 100 μm, applies to panels (a)–(c). (d) Enlargement of region enclosed by dashed rectangle in (a). The FMRF-NH<sub>2</sub> antibody produced an anterior-to-posterior gradient in labeling intensity. Calibration bar = 50 μm. (e) Labeling of *Bgl-FaRP1* mRNA also exhibited an anterior-to-posterior gradient in intensity in Bgp neurons. Calibration bar = 50 μm. (f) Enlarged image of the posterior *Bgl-FaRP2/3* cluster. The neurons in this group give rise to axons (arrowheads) that project in the anterior direction, toward the left pleural-parietal connective. Calibration bar = 50 μm [Color figure can be viewed at [wileyonlinelibrary.com](http://wileyonlinelibrary.com)]

ganglia and the B group of the parietal ganglia (de Lange, Joosse, & van Minnen, 1998; El Filali et al., 2015; van Golen et al., 1995). Whether the male mating system of *Biomphalaria* is innervated by central neurons that express the *Bgl-FaRP2/3* heptapeptides remains uncertain, as FMRF-NH<sub>2</sub>-li projections to the penial nerve from the pleural or parietal ganglia were not observed (Figure 6). Moreover, *Bgl-FaRP2/3* immunoreactive neurons were not detected in the left pleural ganglion or the parietal B group (Figures 10 and 11).

### 4.3 | Feeding system

Early studies showed that micromolar concentrations of FMRF-NH<sub>2</sub> suppressed the feeding motor central pattern generators of *H. trivolis*, *A. californica*, and *L. stagnalis* (Kyriakides & McCrohan, 1989; Murphy et al., 1985; Sossin et al., 1987). In the feeding system of

*Aplysia*, FMRF-NH<sub>2</sub> also modulates transmitter release at the neuromuscular junctions of intrinsic buccal muscles (Church et al., 1993; Fox & Lloyd, 2001; Keating & Lloyd, 1999).

A single *Bgl-FaRP1*-li neuron was labeled on the ventral surface of each buccal hemiganglion, as observed previously in *L. stagnalis* (Santama et al., 1993; Voronezhskaya & Elekes, 2003). While a few buccal FMRF-NH<sub>2</sub>-li cells were labeled by neither the *Bgl-FaRP1* or the *Bgl-FaRP2/3* antibodies (Figure 7), the preponderant agreement between FMRF-NH<sub>2</sub>-like and precursor-specific labeling (Figures 4 and 9–12) supports the utility of FMRF-NH<sub>2</sub> antibodies for localizing bona fide FMRF-NH<sub>2</sub> neurons in gastropods (e.g., Acker et al., 2019; Boer et al., 1980; Cardot & Fellman, 1983; Cooke & Gelperin, 1988; Elekes & Ude, 1994; Lloyd et al., 1987; Schot & Boer, 1982). Some caution is required, however, as a large and diverse family of RF-NH<sub>2</sub> peptides (FMRF-NH<sub>2</sub>-like peptides; FLPs) is expressed in mollusks (see Dockray, 2004; Espinoza et al., 2001; Walker et al., 2009; Zatylny-Gaudin & Favrel, 2014). The presence of LFRF-NH<sub>2</sub> peptides



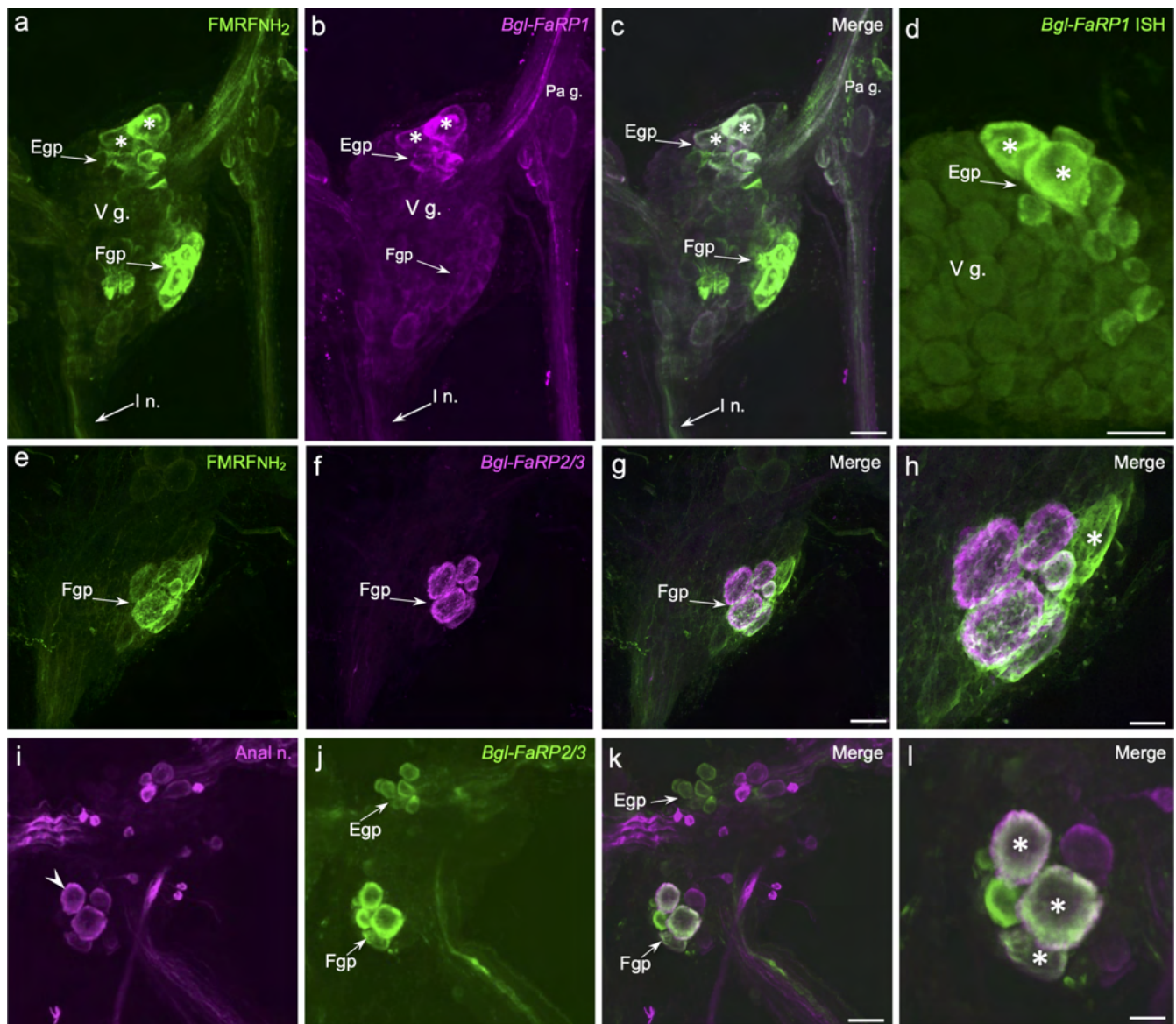


**FIGURE 12** FMRF-NH<sub>2</sub>-li immunoreactivity in the visceral ganglion of *Biomphalaria glabrata*. (a) FMRF-NH<sub>2</sub>-li cells in the visceral ganglion were located in the anterolateral E group (Egp) or the posterolateral F group (Fgp). The two most anterior cells in the Egp (asterisks) were larger than the other neurons in the cluster. FMRF-NH<sub>2</sub>-li fibers were observed in the intestinal nerve (I n.). (b) Egp cells were strongly labeled with the antibody specific for the *Bgl-FaRP1* precursor. Weak immunoreactivity, comparable to that observed in the right parietal ganglion (Pa g.) was also present in the region of the Fgp. (c) Overlay of panels (a) and (b) confirmed *Bgl-FaRP1* labeling of the Egp cells. Calibration bar = 50  $\mu$ m, applies to panels (a)–(c). (d) In situ hybridization with the *Bgl-FaRP1* probe labeled the Egp cells. The hybridization signal in the two largest anterior cells (asterisks) was stronger than in the rest of the Egp. Calibration bar = 50  $\mu$ m. (e) FMRF-NH<sub>2</sub>-li neurons in the Fgp of another *B. glabrata* specimen. (f) FMRF-NH<sub>2</sub>-li neurons in the Fgp were labeled by the *Bgl-FaRP2/3* antibody. (g) An overlay of panels (e) and (f) showed that four to five FMRF-NH<sub>2</sub>-li neurons in the Fgp were labeled by the *FaRP2/3* antibody. Calibration bar = 50  $\mu$ m, applies to panels (e)–(g). (h) Enlargement of Fgp confirmed that five FMRF-NH<sub>2</sub>-li neurons in the Fgp were marked with the *FaRP2/3* antibody. One FMRF-NH<sub>2</sub>-li neurons that was not labeled is marked by an asterisk. Calibration bar = 20  $\mu$ m. (i) Retrograde labeling of the anal nerve filled neurons in the region of the Fgp (arrowhead). (j) The *FaRP2/3* antibody labeled neurons in the Fgp and the Egp. (k) Overlay of panels (i) and (j) showed that most, but not all of the neurons in the Fgp that were stained by the anal nerve backfill were also *FaRP2/3* immunoreactive. Calibration bar = 50  $\mu$ m, applies to panels (i)–(k). (l) Enlargement of the Fgp shows that *FaRP2/3* immunoreactive neurons project to the anal nerve (white, asterisks). Other cells in the Fgp were backfilled but not immunoreactive (magenta) or immunoreactive but not backfilled (green). Calibration bar = 20  $\mu$ m [Color figure can be viewed at [wileyonlinelibrary.com](http://wileyonlinelibrary.com)]

in gastropod feeding networks could contribute to the occurrence of FMRF-NH<sub>2</sub>-li buccal neurons that were not labeled by the SEEPTY or acidic peptide antibodies (Hoek et al., 2005; Vilim et al., 2010).

In gastropods, buccal motor circuits are regulated by a small number of CBIs that are mainly located near the origin of each cerebral-buccal connective (Delaney & Gelperin, 1990; Gillette et al., 1978;



Rosen et al., 1991). Peptidergic signaling by CBIs can achieve coordinated circuit-level modulation of the buccal CPG network (McCrohan & Croll, 1997; Sweedler et al., 2002; Xin et al., 1999). In *L. stagnalis* and *H. trivolis*, the buccal feeding circuit is also regulated by a FMRF-NH<sub>2</sub>-li neuron that projects from the pleural ganglia (Alania et al., 2004; Murphy, 1990). Our observations indicate that one ipsilateral CBI in *Biomphalaria* spp. expresses FMRF-NH<sub>2</sub> (Figure 8(d–f)). To date, projections from pleural neurons have not been observed in retrograde labeling of the *Biomphalaria* C-b c., but the presence of such projections merits further inquiry.

In the buccal ganglia of *Aplysia*, FMRF-NH<sub>2</sub> is present in both motor neurons and sensory neurons (Church & Lloyd, 1991; Vilim et al., 2010). It is a major constituent of the peptide complement transported from the buccal to the cerebral ganglia, leading to the proposal that it participates in signaling by buccal-cerebral interganglionic projections (Lloyd, 1989). Our observations indicate that at least some of the FMRF-NH<sub>2</sub>-li buccal-cerebral projections in *Biomphalaria* snails originate from BCIs that decussate in both ganglia in a circuitous route to their hemiganglion of origin (Figure 8(g–i)). Retrograde labeling should enable a detailed analysis of ipsilateral versus contralateral peptidergic projections between the cerebral and buccal ganglia.

#### 4.4 | Cardiorespiratory system

As observed in *L. stagnalis*, the *Bgl-FaRP2/3* heptapeptide precursors were limited to the visceral and parietal ganglia that control the cardiac and respiratory systems (Santama et al., 1996). While neurons expressing the *Bgl-FaRP1* and *Bgl-FaRP2/3* were intermingled within the E and F groups of the visceral ganglion (Figure 12), the A group of *Bgl-FaRP2/3* expressing neurons in the left parietal ganglion was distinct from the B group (Figure 11). In comparison to *L. stagnalis*, lower numbers of neurons expressing both precursors were detected in the E, F, and B groups of the visceral and left parietal ganglia of *Biomphalaria*, possibly reflecting species differences or a lower sensitivity of the antibodies used in this study.

Early studies demonstrated an increased heart rate in *Biomphalaria* snails that were infected by *S. mansoni* (Lee & Cheng, 1970; Williams & Gilbertson, 1983a, 1983b). In view of the known involvement of identified FaRP tetrapeptide- and heptapeptide-containing neurons in the cardiac system of *L. stagnalis*, such enhanced heart rates may reflect increased signaling by this peptide family. Two neurons within the visceral ganglion E group of *L. stagnalis* express the tetrapeptide precursor and act as cardiac motor neurons (Buckett, Peters, & Benjamin, 1990; Buckett, Peters, Dockray, et al., 1990; Schot et al., 1983). The two most anterior neurons in the E group of *Biomphalaria* spp. were notably larger (Figure 12(a–d)) and may correspond to the E heart excitor ( $E_{he}$ ) neurons of *Limnaea* (Buckett, Peters, & Benjamin, 1990; Buckett, Peters, Dockray, et al., 1990).

A few neurons in the E cluster were labeled with the *Bgl-FaRP2/3*-specific antibody (Figure 12(j)). One heptapeptide containing

cell in the Egg of *L. stagnalis*, termed the VWI, participates in the central circuits that control both respiratory and cardiac activity (Buckett, Peters, & Benjamin, 1990; Buckett, Peters, Dockray, et al., 1990; Syed et al., 1990). While SDPFLRF-NH<sub>2</sub> and GDPFLRF-NH<sub>2</sub> mimic the inhibitory actions that VWI exerts on its central follower neurons in these circuits, SKPYMRF-NH<sub>2</sub> can produce excitatory responses (Kellett et al., 1994; Skingsley et al., 1993). In *Biomphalaria*, the potential to generate heptapeptide transcripts that encode both GDPFLRF-NH<sub>2</sub> and SKPYMRF-NH<sub>2</sub> (*Bgl-FaRP2*) or only GDPFLRF-NH<sub>2</sub> (*Bgl-FaRP3*) could enable heptapeptide containing cells to generate purely inhibitory versus mixed inhibitory/excitatory postsynaptic actions.

#### 4.5 | Future directions: Host FaRPs and the schistosome life cycle

Previous investigations have shown that parasitism by schistosomes can alter FMRF-NH<sub>2</sub> levels in the gastropod CNS. In *L. stagnalis*, increased expression of the tetrapeptide message was measured as early as 1.5 h postinfection by *T. ocellata* (Hoek et al., 1997). Expression remained elevated throughout the 8-week chronology of infection. In *B. glabrata*, FMRF-NH<sub>2</sub> concentrations were increased at 12 days postinfection with *S. mansoni*, when the levels of most neuropeptides were reduced (Wang et al., 2017). It was proposed that increased FMRF-NH<sub>2</sub> levels could reflect enhanced metabolic activity during the prepatent phase of infection (Wang et al., 2017).

In the present study, a wide range of signaling intensities was observed between and within individual ganglia and cell clusters. Such spectra were observed for the *Bgl-FaRP1* and *Bgl-FaRP2/3* precursors and appeared to agree with previous reports in other species (Bright et al., 1993; Santama et al., 1993). Moving forward, the ability to obtain reproducible and correlated histological measures of FaRP gene expression and neuropeptide levels should present opportunities to quantify the impact of infection on this neuropeptide family at the level of specific cell clusters and individual identified neurons.

Finally, neuropeptide signaling systems provide opportunities for identification of novel molecular targets for pesticide and parasiticide drug development (Geary & Maule, 2010; Maule et al., 2002; McVeigh et al., 2011). In contrast to the classical neurotransmitter systems that are presently common targets for pest control, some neuropeptides and their receptors are limited to specific invertebrate clades, reducing concerns of vertebrate toxicity (Mousley et al., 2005; Martin & Robertson, 2010; McVeigh et al., 2012). The FMRF-NH<sub>2</sub> family of neuropeptides has been intensively studied as a target for drug development, due to its pervasive role in the behavior and neuromuscular physiology of major arthropod and helminth parasites and pests (Mousley et al., 2004; McVeigh et al., 2005; McVeigh et al., 2009). If increased FaRP expression in their gastropod intermediate hosts is required for schistosome survival or proliferation, interventions that prevent or reduce such responses could decrease infection of their mammalian definitive hosts.

## ACKNOWLEDGMENTS

Supported by the National Institutes of Health: U54 MD007600 (RCMI), P20 GM103642 (COBRE), Grant Number: P20 GM103475 (INBRE); National Science Foundation: DBI-0932955, HRD-1137725, OISE-1545803, and DBI-1337284; National Academy of Sciences (NAS; USA) - Science and Technology Development Fund (STDF, Egypt) Joint Fund: 2000007152 (USA) and USC17-188 (Egypt). Imaging support was provided by Dr Dina Bracho, UPR COBRE Center for Neuroplasticity, Neuroimaging and Electrophysiology Facility (NIEF). This article is derived from the subject data funded in whole or part by NAS and USAID. Any opinions, findings, conclusions, or recommendations expressed are those of the authors alone, and do not necessarily reflect the views of USAID or NAS.

## CONFLICT OF INTEREST

The authors declare no conflict of interest.

## AUTHOR CONTRIBUTIONS

**Solymar Rolón-Martínez:** Conducted anatomical experiments (*B. glabrata* and *B. alexandrina*), analyzed data. **Mohamed R. Habib:** Conducted anatomical experiments (*B. alexandrina*), analyzed data. **Tamer A. Mansour:** Generated and analyzed *B. glabrata* and *B. alexandrina* transcriptomes. **Manuel Díaz-Ríos:** Generated *B. glabrata* transcriptomes. **Joshua J. C. Rosenthal:** Generated *B. glabrata* transcriptomes. **Xiao-Nong Zhou:** Provided oversight for anatomical experiments (*B. alexandrina*). **Roger P. Croll:** Conceived analysis and interpreted data. **Mark W. Miller:** Conceived and designed analysis. All authors participated in drafting the article. All authors reviewed and approved its content.

## PEER REVIEW

The peer review history for this article is available at <https://publons.com/publon/10.1002/cne.25195>.

## DATA AVAILABILITY STATEMENT

Data are available from the corresponding author upon request. The sequence data files cited in this article have been uploaded to the NCBI Sequence Read Archive as part of Bioproject PRJNA730876 (<https://www.ncbi.nlm.nih.gov/bioproject/PRJNA730876>).

## ORCID

Roger P. Croll  <https://orcid.org/0000-0002-9846-0923>

Mark W. Miller  <https://orcid.org/0000-0002-1237-9631>

## REFERENCES

- Acker, M. J., Habib, M. R., Beach, G. A., Doyle, J. M., Miller, M. W., & Croll, R. P. (2019). An immunohistochemical analysis of peptidergic neurons apparently associated with reproduction and growth in *Biomphalaria alexandrina*. *General and Comparative Endocrinology*, 280, 1–8.
- Adema, C. M., Hillier, L. W., Jones, C. S., Loker, E. S., Knight, M., Minx, P., Oliveira, G., Raghavan, N., Shedlock, A., do Amaral, L. R., Arican-Goktas, H. D., Assis, J. G., Baba, E. H., Baron, O. L., Bayne, C. J., Bickham-Wright, U., Biggar, K. K., Blouin, M., Bonning, B. C., ... Wilson, R. K. (2017). Whole genome analysis of a schistosomiasis-transmitting freshwater snail. *Nature Communications*, 8, 15451. <https://doi.org/10.1038/ncomms15451>
- Ahn, S.-J., Martin, R., Rao, S., & Choi, M.-Y. (2017). Neuropeptides predicted from the transcriptome analysis of the gray garden slug *Deroceras reticulatum*. *Peptides*, 93, 51–65. <https://doi.org/10.1016/j.peptides.2017.05.005>
- Alevizos, A., Bailey, C. H., Chen, M., & Koester, J. (1989). Innervation of vascular and cardiac muscle of *Aplysia* by multimodal motoneuron L7. *Journal of Neurophysiology*, 61, 1053–1063. <https://doi.org/10.1152/jn.1989.61.5.1053>
- Alania, M., Sakharov, D. A., & Elliott, C. J. H. (2004). Multilevel inhibition of feeding by a peptidergic pleural interneuron in the mollusc *Lymnaea stagnalis*. *The Journal of Comparative Physiology A*, 190, 379–390.
- Almagro Armenteros, J. J., Tsirigos, K. D., Sønderby, C. K., Petersen, T. N., Winther, O., Brunak, S., von Heijne, G., & Nielsen, H. (2019). SignalP 5.0 improves signal peptide predictions using deep neural networks. *Nature Biotechnology*, 37, 420–423.
- Altschul, S. F., Gish, W., Miller, W., Myers, E. W., & Lipman, D. J. (1990). Basic local alignment search tool. *Journal of Molecular Biology*, 215, 403–410.
- Austin, T., Weiss, S., & Lukowiak, K. (1983). FMRFamide effects on spontaneous and induced contractions of the anterior gizzard in *Aplysia*. *Canadian Journal of Physiology and Pharmacology*, 61, 949–953.
- Baux, G., Fossier, P., Trudeau, L. E., & Tauc, L. (1992). Presynaptic receptors for FMRFamide, histamine and buccalin regulate acetylcholine release at a neuro-neuronal synapse of *Aplysia* by modulating N-type  $Ca^{2+}$  channels. *The Journal of Physiology*, 86, 3–13.
- Beach, G. A., Habib, M. R., El Hiani, Y., Miller, M. W., & Croll, R. P. (2019). Localization of keyhole limpet hemocyanin-like immunoreactivity in the nervous system of *Biomphalaria alexandrina*. *Journal of Neuroscience Research*, 97, 1469–1482. <https://doi.org/10.1002/jnr.24497>
- Benjamin, P. R., & Burke, J. F. (1994). Alternative mRNA splicing of the FMRFamide gene and its role in neuropeptidergic signalling in a defined neural network. *BioEssays*, 16, 335–342. <https://doi.org/10.1002/bies.950160508>
- Benjamin, P. R., & Winlow, W. (1981). The distribution of three wide-acting inputs to identified neurons in the isolated brain of *Lymnaea stagnalis*. *Comparative Biochemistry & Physiology*, 70A, 293–307.
- Boer, H. H., Schot, L. P., Veenstra, J. A., & Reichelt, D. (1980). Immunocytochemical identification of neural elements in the central nervous systems of a snail, some insects, a fish, and a mammal with an antiserum to the molluscan cardio-excitatory tetrapeptide FMRF-amide. *Cell and Tissue Research*, 213, 21–27.
- Bolger, A. M., Lohse, M., & Usadel, B. (2014). Trimmomatic: A flexible trimmer for Illumina sequence data. *Bioinformatics*, 30, 2114–2120. <https://doi.org/10.1093/bioinformatics/btu170>
- Brezden, B. L., Benjamin, P. R., & Gardner, D. R. (1991). The peptide FMRFamide activates a divalent cation-conducting channel in heart muscle cells of the snail *Lymnaea stagnalis*. *Journal of Physiology*, 443, 727–738.
- Brezina, V., Eckert, R., & Erxleben, C. (1987). Suppression of calcium current by an endogenous neuropeptide in neurones of *Aplysia californica*. *Journal of Physiology*, 388, 565–595.
- Bright, K., Kellett, E., Saunders, S. E., Brierley, M., Burke, J. F., & Benjamin, P. R. (1993). Mutually exclusive expression of alternatively spliced FMRFamide transcripts in identified neuronal systems of the snail *Lymnaea*. *Journal of Neuroscience*, 6, 2719–2729.
- Brussaard, A. B., Kits, K. S., ter Maat, A., van Minnen, J., & Moed, P. J. (1988). Dual inhibitory action of FMRFamide on neurosecretory cells controlling egg laying behavior in the pond snail. *Brain Research*, 447, 35–51.
- Buckett, K. J., Peters, M., & Benjamin, P. R. (1990). Excitation and inhibition of the heart of the snail *Lymnaea* by non-FMRFamidergic motoneurons. *Journal of Neurophysiology*, 63, 1436–1447.

- Buckett, K. J., Peters, M., Dockray, J., van Minnen, J., & Benjamin, P. R. (1990). Regulation of heartbeat in *Lymnaea* by motoneurons containing FMRFamide-like peptides. *The Journal of Neurophysiology*, 63, 1426–1435.
- Bullock, A. G., Price, D. A., Murphy, A. D., Lee, T. D., & Bowes, H. N. (1988). FMRFamide peptides in *Helisoma*: Identification and physiological actions at a peripheral synapse. *Journal of Neuroscience*, 8, 3459–3469.
- Cardot, J., & Fellman, D. (1983). Immunofluorescent evidence of an FMRFamide-like peptide in the peripheral nervous system of the gastropod mollusc *Helix aspersa*. *Neuroscience Letters*, 43, 167–172.
- Chase, R. (2002). *Behavior and its neural control in gastropod molluscs*. Oxford University Press.
- Church, P. J., & Lloyd, P. E. (1991). Expression of diverse neuropeptide cotransmitters by identified motor neurons in *Aplysia*. *Journal of Neuroscience*, 11, 618–25. <https://doi.org/10.1523/JNEUROSCI.11-03-00618.1991>.
- Church, P., Whim, M., & Lloyd, P. (1993). Modulation of neuromuscular transmission by conventional and peptide transmitters released from excitatory and inhibitory motor neurons in *Aplysia*. *The Journal of Neuroscience*, 13, 2790–2800. <https://doi.org/10.1523/jneurosci.13-07-02790.1993>
- Cooke, I. C., & Gelperin, A. (1988). Distribution of FMRFamide-like immunoreactivity in the nervous system of the slug *Limax maximus*. *Cell & Tissue Research*, 253, 69–76. <https://doi.org/10.1007/bf00221741>.
- Cottrell, G. A. (1993). The wide range of actions of the FMRFamide-related peptides and the biological importance of peptidergic messengers. *Experientia Supplementum*, 63, 279–285.
- Cottrell, G. A., Greenberg, M. J., & Price, D. A. (1983). Differential effects of the molluscan neuropeptide FMRFamide and the related Met-enkephalin derivative YGGFMRFa on the tentacle retractor muscle. *Comparative Biochemistry & Physiology*, 75C, 373–375.
- Cottrell, G. A., Price, D. A., Doble, K. E., Hettle, S., Sommerville, J., & MacDonald, M. (1992). Identified *Helix* neurons: Mutually exclusive expression of the tetrapeptide and heptapeptide members of the FMRFamide family. *The Biological Bulletin*, 183, 113–122. <https://doi.org/10.2307/1542412>
- Croll, R. P., & van Minnen, J. (1992). Distribution of the peptide Ala-Pro-Gly-Trp-NH<sub>2</sub> (APGWamide) in the nervous system and periphery of the snail *Lymnaea stagnalis* as revealed by immunocytochemistry and *in situ* hybridization. *The Journal of Comparative Neurology*, 324, 567–574. <https://doi.org/10.1002/cne.903240409>
- Crusoe, M. R., Alameldin, H. F., Awad, S., et al. (2015). The khmer software package: Enabling efficient nucleotide sequence analysis [version 1; peer review: 2 approved, 1 approved with reservations]. *F1000Research*, 4, 900. <https://doi.org/10.12688/f1000research.6924.1>
- Cummins, S. F., Tollenaere, A., Degnan, B. M., & Croll, R. P. (2011). Molecular analysis of two FMRFamide-encoding transcripts expressed during the development of the tropical abalone *Haliotis asinina*. *The Journal of Comparative Neurology*, 519, 2043–2059.
- de Boer, P. A. C. M., Jansen, R. F., & ter Maat, A. (1996). Copulation in the hermaphrodite snail *Lymnaea stagnalis*: A review. *Invertebrate Reproduction & Development*, 30, 167–176.
- de Jong-Brink, M. (1995). How schistosomes profit from the stress responses they elicit in their hosts. *Advances in Parasitology*, 35, 177–256.
- de Jong-Brink, M., Bergamin-Sassen, M., & Solis Soto, M. (2001). Multiple strategies of schistosomes to meet their requirements in the intermediate snail host. *Parasitology*, 123, S129–S141.
- de Lange, R. P. J., de Boer, P. A. C. M., ter Maat, A., Tensen, C. P., & van Minnen, J. (1998). Transmitter identification in neurons involved in male copulation behavior in *Lymnaea stagnalis*. *The Journal of Comparative Neurology*, 395, 440–449. [https://doi.org/10.1002/\(sici\)1096-9861\(19980615\)395:4<440::aid-cne2>3.0.co;2-1](https://doi.org/10.1002/(sici)1096-9861(19980615)395:4<440::aid-cne2>3.0.co;2-1)
- de Lange, R. P. J., Joosse, J., & van Minnen, J. (1998). Multi-messenger innervation of the male sexual system of *Lymnaea stagnalis*. *The Journal of Comparative Neurology*, 390, 564–577. [https://doi.org/10.1002/\(sici\)1096-9861\(19980126\)390:4<564::aid-cne8>3.0.co;2-z](https://doi.org/10.1002/(sici)1096-9861(19980126)390:4<564::aid-cne8>3.0.co;2-z)
- Delaney, K., & Gelperin, A. (1990). Cerebral interneurons controlling fictive feeding in *Limax maximus*. *The Journal of Comparative Physiology A*, 166, 297–310. <https://doi.org/10.1007/BF00204804>
- Delgado, N., Vallejo, D., & Miller, M. W. (2012). Localization of serotonin in the nervous system of *Biomphalaria glabrata*, an intermediate host for schistosomiasis. *The Journal of Comparative Neurology*, 520, 3236–3255.
- Dockray, G. J. (2004). The expanding family of RFamide peptides and their effects on feeding behavior. *Experimental Physiology*, 89, 229–235.
- El Filali, Z., de Boer, P. A. C. M., Pieneman, A. W., de Lange, R. P. J., Jansen, R. F., ter Maat, A., van der Schors, R. C., Li, K. W., van Straalen, N. M., & Koene, M. (2015). Single-cell analysis of peptide expression and electrophysiology of right parietal neurons involved in male copulation behavior of a simultaneous hermaphrodite. *Invertebrate Neuroscience*, 15, 7.
- Elekes, K., & Ude, J. (1994). Peripheral connections of FMRFamide-like immunoreactive neurons in the snail, *Helix pomatia*: An immunogold electron microscopic study. *Journal of Neurocytology*, 23, 758–769. <https://doi.org/10.1007/bf01268088>
- Elliott, C. J., & Susswein, A. J. (2002). Comparative neuroethology of feeding control in molluscs. *The Journal of Experimental Biology*, 205, 877–896.
- Espinoza, E., Carrigan, M., Thomas, S. G., Shaw, G., & Edison, A. S. (2001). A statistical view of FMRFamide neuropeptide diversity. *Molecular Neurobiology*, 21, 35–56. <https://doi.org/10.1385/mn:21:1:2:035>
- Fisher, J. M., Sossin, W., Newcomb, R., & Scheller, R. H. (1988). Multiple neuropeptides derived from a common precursor are differentially packaged and transported. *Cell*, 54, 813–822. [https://doi.org/10.1016/s0092-8674\(88\)91131-2](https://doi.org/10.1016/s0092-8674(88)91131-2)
- Fong, P. P., Olex, A. L., Farrell, J. E., Majchrzak, R. M., & Muschamp, J. W. (2005). Induction of preputium eversion by peptides, serotonin receptor antagonists, and selective serotonin reuptake inhibitors in *Biomphalaria glabrata*. *Invertebrate Biology*, 124, 296–302. <https://doi.org/10.1111/j.1744-7410.2005.00027.x>
- Fox, L. E., & Lloyd, P. E. (2001). Evidence that post-tetanic potentiation is mediated by neuropeptide release in *Aplysia*. *Journal of Neurophysiology*, 86, 2845–55.
- Geary, T. G., & Maule, A. G. (Eds.). (2010). *Neuropeptide systems as targets for parasite and pest control*. Landes Bioscience and Springer Science + Business Media.
- Gillette, R., Kovac, M. P., & Davis, W. J. (1978). Command neurons in *Pleurobranchaea* receive synaptic feedback from motor networks they excite. *Science*, 199, 798–801.
- Grabherr, M. G., Haas, B. J., Yassour, M., Levin, J. Z., Thompson, D. A., ... Regev, A. (2011). Full-length transcriptome assembly from RNA-seq data without a reference genome. *Nature Biotechnology*, 29, 644–652. <https://doi.org/10.1038/nbt.1883>
- Greenberg, M. J., Payza, K., Nachman, R. J., Holman, G. M., & Price, D. A. (1988). Relationships between the FMRFamide-related peptides and other peptide families. *Peptides*, 9(Suppl 1), 125–135. [https://doi.org/10.1016/0196-9781\(88\)90236-7](https://doi.org/10.1016/0196-9781(88)90236-7)
- Hoek, R. M., Li, K. W., van Minnen, J., Lodder, J. C., de Jong-Brink, M., Smit, A. B., & van Kesteren, R. E. (2005). LFRFamides: A novel family of parasitism-induced RFamide neuropeptides that inhibit the activity of neuroendocrine cells in *Lymnaea stagnalis*. *Journal of Neurochemistry*, 92, 1073–1080. <https://doi.org/10.1111/j.1471-4159.2004.02927.x>
- Hoek, R. M., van Kesteren, R. E., Smit, A. B., de Jong-Brink, M., & Geraerts, W. P. M. (1997). Schistosome parasites directly induce changes in gene expression in the central nervous system of their molluscan host. *Proceedings of the National Academy of Sciences of the United States of America*, 94, 14072–14076.
- Hosaka, M., Nagahama, M., Kim, W. S., Watanabe, T., Hatsuzawa, K., Ikemizu, J., Murakami, K., & Nakayama, K. (1991). Arg-X-Lys/Arg-Arg



- motif as a signal for precursor cleavage catalyzed by furin within the constitutive secretory pathway. *Journal of Biological Chemistry*, 266, 12127–12130.
- Keating, C., & Lloyd, P. E. (1999). Differential modulation of motor neurons that innervate the same muscle but use different excitatory transmitters in *Aplysia*. *Journal of Neurophysiology*, 82, 1759–1767. <https://doi.org/10.1152/jn.1999.82.4.1759>.
- Kellett, E., Saunders, S. E., Li, K. W., Staddon, J. W., Benjamin, P. R., & Burke, J. F. (1994). Genomic organization of the FMRFamide gene in *Lymnaea*: Multiple exons encoding novel neuropeptides. *Journal of Neuroscience*, 14, 6564–6570.
- Koene, J. M., Jansen, R. F., Ter Maat, A., & Chase, R. (2000). A conserved location for the central nervous system control of mating behaviour in gastropod molluscs: evidence from a terrestrial snail. *Journal of Experimental Biology*, 203, 1071–1080.
- Koene, J. M. (2010). Neuro-endocrine control of reproduction in hermaphroditic freshwater snails: Mechanisms and evolution. *Frontiers in Behavioral Neuroscience*, 4, 167. <https://doi.org/10.3389/fnbeh.2010.00167>
- Kupfermann, I. (1974). Dissociation of the appetitive and consummatory phases of feeding behavior in *Aplysia*: A lesion study. *Behavioral Biology*, 10, 89–97.
- Kyriakides, M. A., & McCrohan, C. R. (1989). Effect of putative neuromodulators on rhythmic buccal motor output in *Lymnaea stagnalis*. *Journal of Neurobiology*, 20, 635–650. <https://doi.org/10.1002/neu.480200704>
- Lee, F. O., & Cheng, T. C. (1970). Increased heart rate in *Biomphalaria glabrata* parasitized by *Schistosoma mansoni*. *Journal of Invertebrate Pathology*, 16, 148–149.
- Lehman, H. K., & Price, D. A. (1987). Localization of FMRFamide-like peptides in the snail *Helix aspersa*. *The Journal of Experimental Biology*, 131, 37–53.
- Lehman, H. K., & Greenberg, M. J. (1987). The actions of FMRFamide-like peptides on visceral and somatic muscles of the snail *Helix aspersa*. *Journal of Experimental Biology*, 31, 55–68.
- Lever, J., de Vries, C. M., & Jager, J. C. (1965). On the anatomy of the central nervous system and location of neurosecretory cells in *Australorbis glabratus*. *Malacologia*, 2, 219–230.
- Li, G., & Chase, R. (1995). Correlation of axon projections and peptide immunoreactivity in mesocerebral neurons of the snail *Helix aspersa*. *The Journal of Comparative Neurology*, 353, 9–17.
- Li, K. W., Jiménez, C. R., van Veelen, P. A., & Geraerts, W. P. (1994). Processing and targeting of a molluscan egg-laying peptide prohormone as revealed by mass spectrometric peptide fingerprinting and peptide sequencing. *Endocrinology*, 134, 1812–1819. <https://doi.org/10.1210/endo.134.4.81377747>
- Li, W., & Godzik, A. (2006). CD-HIT: A fast program for clustering and comparing large sets of protein or nucleotide sequences. *Bioinformatics*, 22, 1658–1659.
- Linacre, A., Kellett, E., Saunders, S. E., Bright, K., Benjamin, P. R., & Burke, J. F. (1990). Cardioactive neuropeptide Phe-Met-Arg-Phe-NH<sub>2</sub> (FMRFamide) and novel related peptides are encoded in multiple copies by a single gene in the snail *Lymnaea stagnalis*. *The Journal of Neuroscience*, 10, 412–419.
- Lloyd, P., Frankfurt, M., Stevens, P., Kupfermann, I., & Weiss, K. (1987). Biochemical and immunocytological localization of the neuropeptides FMRFamide, SCP<sub>A</sub>, SCP<sub>B</sub>, to neurons involved in the regulation of feeding in *Aplysia*. *The Journal of Neuroscience*, 7, 1123–1132. <https://doi.org/10.1523/jneurosci.07-04-01123.1987>
- Lloyd, P. E. (1989). Interganglionic axonal transport of neuropeptides in *Aplysia*. *Journal of Neuroscience*, 9, 3243–3249.
- Lutz, E. M., MacDonald, M., Hettle, S., Price, D. A., Cottrell, G. A., & Somerville, J. (1992). Structure of cDNA clones and genomic DNA FMRFamide-related peptides (FaRPs) in *Helix*. *Molecular and Cellular Neuroscience*, 3, 373–382.
- MacDonald, M., Lutz, E. M., Lesser, W., Cottrell, G. A., & Somerville, J. (1994). Expression of mRNA encoding FMRFamide-related peptides (FaRPs) in the nervous system of *Helix aspersa*. *Molecular and Cellular Neuroscience*, 5, 23–34.
- Mackey, S. L., Glanzman, D. L., Small, S. A., Dyke, A. M., Kandel, E. R., & Hawkins, R. D. (1987). Tail shock produces inhibition as well as sensitization of the siphon-withdrawal reflex of *Aplysia*: Possible behavioral role for presynaptic inhibition mediated by the peptide Phe-Met-Arg-Phe-NH<sub>2</sub>. *Proceedings of the National Academy of Sciences of the United States of America*, 84, 8730–8734. <https://doi.org/10.1073/pnas.84.23.8730>
- Maldonado, J. F., & Perkins, K. W. (1967). *Schistosomiasis in America*. Editorial Científico-Médica.
- Man-Song-Hing, H., Zoran, M. J., Lukowiak, K., & Haydon, P. G. (1989). A neuromodulator of synaptic transmission acts on the secretory apparatus as well as on ion channels. *Nature*, 341, 237–239.
- Martin, R. J., & Robertson, A. P. (2010). Control of nematode parasites with agents acting on neuro-musculature systems: Lessons for neuropeptide ligand discovery. *Advances in Experimental Medicine and Biology*, 692, 138–154.
- Maule, A. G., Mousley, A., Marks, N. J., Day, T. A., Thompson, D. P., Geary, T. G., & Halton, D. W. (2002). Neuropeptide signaling systems - potential drug targets for parasite and pest control. *Current Topics in Medicinal Chemistry*, 2, 733–758.
- McCrohan, C. R., & Croll, R. P. (1997). Characterization of an identified cerebrobuccal neuron containing the neuropeptide APGWamide (Ala-Pro-Gly-Trp-NH<sub>2</sub>) in the snail *Lymnaea stagnalis*. *Invertebrate Neuroscience*, 2, 273–282. <https://doi.org/10.1007/bf02211940>
- McVeigh, P., Leech, S., Mair, G. R., Marks, N. J., Geary, T. G., & Maule, A. G. (2005). Analysis of FMRFamide-like peptide (FLP) diversity in phylum nematoda. *International Journal of Parasitology*, 35, 1043–1060.
- McVeigh, P., Mair, G. R., Atkinson, L., Zamanian, M., Ladurner, P., Novozhilova, E., Marks, N. J., Day, T. A., & Maule, A. G. (2009). Discovery of multiple neuropeptide families in phylum Platyhelminthes. *International Journal of Parasitology*, 39, 1243–1252.
- McVeigh, P., Atkinson, L., Marks, N. J., Mousley, A., Dalzell, J. J., Sluder, A., Hammerland, L., & Maule, A. G. (2012). Parasite neuropeptide biology: Seeding rational drug target selection? *International Journal for Parasitology: Drugs and Drug Resistance*, 2, 76–91.
- Mousley, A., Marks, N. J., & Maule, A. G. (2004). Neuropeptide signalling: A repository of targets for novel endectocides? *Trends in Parasitology*, 20, 482–487.
- Mousley, A. I., Maule, A. G., Halton, D. W., & Marks, N. J. (2005). Interphyla studies on neuropeptides: The potential for broad-spectrum anthelmintic and/or endectocide discovery. *Parasitology*, 131, S143–S167.
- Murphy, A. D. (1990). An identified pleural ganglion interneuron inhibits patterned motor activity in the buccal ganglia of the snail, *Helisoma*. *Brain Research*, 525, 300–303.
- Murphy, A. D. (2001). The neuronal basis of feeding in the snail, *Helisoma*, with comparisons to selected gastropods. *Progress in Neurobiology*, 63, 383–408.
- Murphy, A. D., Lukowiak, K., & Stell, W. K. (1985). Peptidergic modulation of patterned motor activity in identified neurons of *Helisoma*. *Proceedings of the National Academy of Sciences of the United States of America*, 82, 7140–7144. <https://doi.org/10.1073/pnas.82.20.7140>
- Muschamp, J. W., & Fong, P. P. (2001). Effects of the serotonin receptor ligand methiothepin on reproductive behavior of the freshwater snail *Biomphalaria glabrata*: Reduction of egg laying and induction of penile erection. *Journal of Experimental Zoology*, 289, 202–207. [https://doi.org/10.1002/1097-010x\(20010215\)289:3<202::aid-jez7>3.0.co;2-b](https://doi.org/10.1002/1097-010x(20010215)289:3<202::aid-jez7>3.0.co;2-b)
- Petersen, T. N., Brunak, S., von Heijne, G., & Henrik Nielsen, H. (2011). SignalP 4.0: Discriminating signal peptides from transmembrane regions. *Nature Methods*, 8, 785–786.

- Price, D. A., & Greenberg, M. J. (1977). The structure of a molluscan cardioexcitatory neuropeptide. *Science*, 197, 670–671.
- Price, D. A., & Greenberg, M. J. (1989). The hunting of FaRPs: The distribution of FMRFamide-related peptides. *Biological Bulletin*, 177, 198–205.
- Proudfoot, N. J., & Brownlee, G. G. (1976). 3' Non-coding region sequences in eukaryotic messenger RNA. *Nature*, 263, 211–214.
- Rollinson, D., & Chappell, L. H. (2002). *Flukes and snails revisited*. Cambridge University Press.
- Rosa-Casillas, M., Méndez de Jesús, P., Vicente Rodríguez, L. C., Habib, M. R., Croll, R. P., & Miller, M. W. (2021). Identification and localization of a gonadotropin-releasing hormone-related neuropeptide in *Biomphalaria*, an intermediate host for schistosomiasis. *Journal of Comparative Neurology*, 529, 2347–2361. <https://doi.org/10.1002/cne.25099>.
- Rosen, S. C., Teyke, T., Miller, M. W., Weiss, K. R., & Kupfermann, I. (1991). Identification and characterization of cerebral-to-buccal interneurons implicated in the control of motor programs associated with feeding in *Aplysia*. *Journal of Neuroscience*, 11, 3630–3655.
- Santama, N., & Benjamin, P. R. (2000). Gene expression and function of FMRFamide-related neuropeptides in the snail *Lymnaea*. *Microscopy Research and Technique*, 49, 547–556.
- Santama, N., Benjamin, P. R., & Burke, J. F. (1995). Alternative RNA splicing generates diversity of neuropeptide expression in the brain of the snail *Lymnaea*: *In situ* analysis of mutually exclusive transcripts of the FMRF amide gene. *European Journal of Neuroscience*, 7, 65–76. <https://doi.org/10.1111/j.1460-9568.1995.tb01021.x>
- Santama, N., Li, K. W., Bright, K. E., Yeoman, M., Geraerts, W. P. M., Benjamin, P. R., & Burke, J. F. (1993). Processing of the FMRFamide precursor protein in the snail *Lymnaea stagnalis*: Characterization and neuronal localization of a novel peptide, 'SEEPLY'. *European Journal of Neuroscience*, 5, 1003–1016.
- Santama, N., Li, K. W., Geraerts, W. P., Benjamin, P. R., & Burke, J. F. (1996). Post-translational processing of the alternative neuropeptide precursor encoded by the FMRFamide gene in the pulmonate snail *Lymnaea stagnalis*. *European Journal of Neuroscience*, 8, 968–977.
- Saunders, S. E., Bright, K., Kellett, E., Benjamin, P. R., & Burke, J. F. (1991). Neuropeptides Gly-Asp-Pro-Phe-Leu-Arg-Phe-amide (GDPFLRFamide) and Ser-Asp-Pro-Phe-Leu-Arg-Phe-amide (SDPFLRFamide) are encoded by an exon 3' to Phe-Met-Arg-Phe NH<sub>2</sub> (FMRFamide) in the snail *Lymnaea stagnalis*. *The Journal of Neuroscience*, 11, 740–745.
- Saunders, S. E., Kellett, E., Bright, K., Benjamin, P. R., & Burke, J. F. (1992). Cell-specific alternative RNA splicing of an FMRFamide gene transcript in the brain. *The Journal of Neuroscience*, 12, 1033–1039.
- Schot, L. P. C., & Boer, H. H. (1982). Immunocytochemical demonstration of peptidergic cells in the pond snail *Lymnaea stagnalis* with an antiserum to the molluscan cardioactive tetrapeptide FMRF-amide. *Cell and Tissue Research*, 225, 347–354.
- Schot, L. P. C., Boer, H. H., & Wijdenes, J. (1983). Localization of neurons innervating the heart innervating the heart of *Lymnaea stagnalis* studied immunocytochemically with anti-FMRFamide and anti-vasotocin. In *Molluscan neuroendocrinology* (pp. 203–208). Royal Netherlands Academy of Arts and Sciences.
- Senatore, A., Edirisinghe, N., & Katz, P. S. (2015). Deep mRNA sequencing of the *Tritonia diomedea* brain transcriptome provides access to gene homologues for neuronal excitability, synaptic transmission and peptidergic signalling. *PLoS One*, 10, e0118321. <https://doi.org/10.1371/journal.pone.0118321>
- Seppely, M., Manni, M., & Zdobnov, E. M. (2019). BUSCO: Assessing genome assembly and annotation completeness. In M. Kollmar (Ed.), *Gene prediction. Methods in molecular biology* (Vol. 1962). Humana.
- Skingsley, D. R., Bright, K., Santama, N., van Minnen, J., Brierley, M. J., Burke, J. F., & Benjamin, P. R. (1993). A molecularly defined cardiorespiratory interneuron expressing SDPFLRFamide/GDPFLRFamide in the snail *Lymnaea*: Monosynaptic connections and pharmacology. *Journal of Neurophysiology*, 69, 915–927. <https://doi.org/10.1152/jn.1993.69.3.915>
- Smit, A. B., van Kesteren, R. E., Spijker, S., van Minnen, J., van Golen, F. A., Jiménez, C. R., & Li, K. W. (2003). Peptidergic modulation of male sexual behavior in *Lymnaea stagnalis*: Structural and functional characterization of -FVamide neuropeptides. *Journal of Neurochemistry*, 87(5), 1245–1254. <https://doi.org/10.1046/j.1471-4159.2003.02086.x>
- Sossin, W., Kirk, M., & Scheller, R. (1987). Peptidergic modulation of neuronal circuitry controlling feeding in *Aplysia*. *The Journal of Neuroscience*, 7, 671–681. <https://doi.org/10.1523/jneurosci.07-03-00671.1987>
- Sossin, W. S., Sweet-Cordero, A., & Scheller, R. H. (1990). Dale's hypothesis revisited: Different neuropeptides derived from a common prohormone are targeted to different processes. *Proceedings of the National Academy of Sciences of the United States of America*, 87, 4845–4848. <https://doi.org/10.1073/pnas.87.12.4845>
- Sweedler, J. V., Li, L., Rubakhin, S. S., Alexeeva, V., Dembrow, N. C., Dowling, O., ... Vilim, F. S. (2002). Identification and characterization of the feeding circuit-activating peptides, a novel neuropeptide family of *Aplysia*. *The Journal of Neuroscience*, 22, 7797–7808. <https://doi.org/10.1523/jneurosci.22-17-07797.2002>
- Sweet-Cordero, A., Fisher, J. M., Sossin, W., Newcomb, R., & Scheller, R. H. (1990). Subcellular fractionation of prohormone processing products in the bag cell neurons. *Journal of Neurochemistry*, 55, 1933–1941. <https://doi.org/10.1111/j.1471-4159.1990.tb05779.x>
- Syed, N. I., Bulloch, A. G., & Lukowiak, K. (1990). *In vitro* reconstruction of the respiratory central pattern generator of the mollusk *Lymnaea*. *Science*, 250, 282–285. <https://doi.org/10.1126/science.2218532>
- Syed, N. I., & Winlow, W. (1991). Coordination of locomotor and cardiorespiratory networks of *Lymnaea stagnalis* by a pair of identified interneurons. *Journal of Experimental Biology*, 158, 37–62.
- Taussig, R., & Scheller, R. H. (1986). The *Aplysia* FMRFamide gene encodes sequences related to mammalian brain peptides. *DNA*, 5, 453–461.
- Toledo, R., & Fried, B. (Eds.). (2011). *Biomphalaria snails and larval trematodes*. Springer Science+Business Media.
- van Duivenboden, Y. A., & ter Maat, A. (1988). Mating behaviour of *Lymnaea stagnalis*. *Malacologia*, 28, 23–64.
- van Golen, F. A., Li, K. W., de Lange, R. P. J., Jespersen, S., & Geraerts, W. P. M. (1995). Mutually exclusive neuronal expression of peptides encoded by the FMRFa gene underlies a differential control of copulation in *Lymnaea*. *The Journal of Biological Chemistry*, 270, 28487–28493.
- Vallejo, D., Habib, M. R., Delgado, N., Vaasjo, L. O., Croll, R. P., & Miller, M. W. (2014). Localization of tyrosine hydroxylase-like immunoreactivity in the nervous systems of *Biomphalaria glabrata* and *Biomphalaria alexandrina*, intermediate hosts for schistosomiasis. *Journal of Comparative Neurology*, 522, 2532–52. <https://doi.org/10.1002/cne.23548>
- Vaasjo, L. O., Quintana, A. M., Habib, M. R., Mendez de Jesus, P. A., Croll, R. P., Miller, M. W. (2018). GABA-like immunoreactivity in *Biomphalaria*: Colocalization with tyrosine hydroxylase-like immunoreactivity in the feeding motor systems of pulmonate snails. *Journal of Comparative Neurology*, 526, 1790–1805. <https://doi.org/10.1002/cne.24448>
- Vilim, F. S., Sasaki, K., Rybak, J., Alexeeva, V., Cropper, E. C., Jing, J., Orekhova, I. V., Brezina, V., Price, D., Romanova, E. V., Rubakhin, S. S., Hatcher, N., Sweedler, J. V., & Weiss, K. R. (2010). Distinct mechanisms produce functionally complementary actions of neuropeptides that are structurally related but derived from different precursors. *The Journal of Neuroscience*, 30, 131–147.
- Voronezhskaya, E. E., & Elekes, K. (2003). Expression of FMRFamide gene encoded peptides by identified neurons in embryos and juveniles of the pulmonate snail *Lymnaea stagnalis*. *Cell and Tissue Research*, 314, 297–313.
- Walker, R. J., Papaioannou, S., & Holden-Dye, L. (2009). A review of FMRFamide- and RFamide-like peptides in metazoa. *Invertebrate Neuroscience*, 9, 111–153. <https://doi.org/10.1007/s10158-010-0097-7>
- Wang, T., Zhao, M., Liang, D., Bose, U., Kaur, S., McManus, D. P., & Cummins, S. F. (2017). Changes in the neuropeptide content of

- Biomphalaria* ganglia nervous system following *Schistosoma* infection. *Parasites & Vectors*, 10, 275. <https://doi.org/10.1186/s13071-017-2218-1>.
- Williams, C. L., & Gilbertson, D. E. (1983a). Altered feeding response as a cause for the altered heartbeat rate and locomotor activity of *Schistosoma mansoni*-infected *Biomphalaria glabrata*. *Journal of Parasitology*, 69, 671–676.
- Williams, C. L., & Gilbertson, D. E. (1983b). Effects of alterations in the heartbeat rate and locomotor activity of *Schistosoma mansoni*-infected *Biomphalaria glabrata* on cercarial emergence. *Journal of Parasitology*, 69, 677–681.
- Worster, B. M., Yeoman, M. S., & Benjamin, P. R. (1998). Matrix-assisted laser desorption/ionization time of flight mass spectrometric analysis of the pattern of peptide expression in single neurons resulting from alternative mRNA splicing of the FMRFamide gene. *European Journal of Neuroscience*, 10, 3498–3507. <https://doi.org/10.1046/j.1460-9568.1998.00361.x>
- Xin, Y., Hurwitz, I., Perrins, R., Evans, C. G., Alexeeva, V., Weiss, K. R., & Kupfermann, I. (1999). Actions of a pair of identified cerebral-buccal interneurons (CBI-8/9) in *Aplysia* that contain the peptide myomodulin. *Journal of Neurophysiology*, 81, 507–520. <https://doi.org/10.1152/jn.1999.81.2.507>
- Zatylny-Gaudin, C., & Favrel, P. (2014). Diversity of the RFamide peptide family in mollusks. *Frontiers in Endocrinology*, 5, 178. <https://doi.org/10.3389/fendo.2014.00178>

**How to cite this article:** Rolón-Martínez, S., Habib, M. R., Mansour, T. A., Díaz-Ríos, M., Rosenthal, J. J. C., Zhou, X.-N., Croll, R. P., & Miller, M. W. (2021). FMRF-NH<sub>2</sub>-related neuropeptides in *Biomphalaria* spp., intermediate hosts for schistosomiasis: Precursor organization and immunohistochemical localization. *Journal of Comparative Neurology*, 1–23. <https://doi.org/10.1002/cne.25195>